13 Zhang M, Zamore PD, Carmo-Fonseca M, Lamond AI, Green MR. Cloning and intracellular localization of the U2 small nuclear ribonucleoprotein auxiliary factor small subunit. *Proc Natl Acad Sci USA* 1992; **89**: 8769–8773.

14 Edmond V, Brambilla C, Brambilla E, Gazzeri S, Eymin B. SRSF2 is required for sodium butyrate-mediated p21(WAF1) induction and premature senescence in human lung carcinoma cell lines. *Cell Cycle* 2011; **10**: 1968–1977.

15 Emanuel PD. Juvenile myelomonocytic leukemia and chronic myelomonocytic leukemia. *Leukemia* 2008; **22**: 1335–1342.

Supplementary Information accompanies the paper on the Leukemia website (http://www.nature.com/leu)

Sequencing histone-modifying enzymes identifies UTX mutations in acute lymphoblastic leukemia

Leukemia (2012) **26,** 1881–1883; doi:10.1038/leu.2012.56

Mutations affecting epigenetic regulators have long been known to have a crucial role in cancer and, in particular, hematological malignancies.[1,2] One of the earliest epigenetic factors described altered in leukemia was the mixed lineage leukemia (*MLL*) protein which is found translocated in 10% of adult acute myeloid leukemia (AML), 30% of secondary AML and >75% of infants with both AML and acute lymphocytic leukemia (ALL). *MLL* is a SET domain-containing protein, which is recruited to many promoters and mediates histone 3 lysine 4 (H3K4) methyltransferase activity, thought to promote gene expression.[3]

In addition to *MLL* fusions, recently, somatic mutations of *UTX* (also known as *KDM6A*), encoding an H3K27 demethylase, were described in multiple hematological malignancies, including multiple myeloma and many types of leukemia cell lines.[4,5] H3K27 methylation is generally thought to cause gene repression. Complimentary to *UTX*, mutations of *EZH2*, a H3K27 methyltransferase, have been reported in both lymphoid and myeloid tumors (Figure 1).[6,7] These mutations lead to altered EZH2 activity and influence H3K27 in tumor cells. Mutations in EZH2, EED and SUZ12, which all cooperate in Polycomb repressive complex 2 have been recently described in early T-cell precursor ALL.[8] Similarly, point mutations affecting the functional jumonji C (jmjC) domain of UTX inactivates its H3K27 demethylase activity. In addition, UTX associates with MLL2 in a multiprotein complex, which promotes H3K4 methylation, and recently *MLL2* has also been found mutated in cancer, further pointing to a common and complex epigenetic deregulation in cancer.[9] In line with the growing evidence for epigenetic regulators as important in tumorigenesis, additional mutations affecting epigenetic regulators such as SETD2, a H3K36 methyltransferase, KDM3B, a H3K9 demethylase, and KDM5C, a H3K4 demethylase, have been reported and are associated with distinct gene expression patterns (Figure 1).[4]

Though the clinical significance of these findings remains to be explored, it is evident that epigenetic deregulation is having an important role in both lymphoid and myeloid leukemogenesis. Furthermore, with novel drugs at hand, such as histone deacetylase inhibitors or demethylating agents that can target and reverse epigenetic alterations, understanding the underlying molecular aberrations is of growing interest.[10] We therefore undertook an effort to examine the prevalence of somatic mutations in genes encoding histone-modifying proteins, in particular, *KDM3B*, *KDM5C*, *UTX*, *MLL2*, *EZH2* and *SETD2*, which previously were reported mutated in cancer.[4,5]

For an initial screen, we analyzed banked diagnostic primary leukemia samples from 44 childhood B-cell ALL and 50 adult AML patients, and, where available, used bone marrow samples obtained in complete remission to validate the somatic nature of the mutations. Samples had been collected with patient/parental informed consent from patients enrolled on Dana–Farber Cancer Institute protocols for childhood ALL (DFCI 00-001 (NCT00165178), DFCI 05-001 (NCT00400946)) or AML treatment protocols of the German-Austrian AML Study Group (AMLSG) for younger adults (AMLSG-HD98A (NCT00146120), AMLSG 07-04 (NCT00151242)), and the study was approved by the IRB of the participating centers.

Using conventional Sanger sequencing of primary leukemia sample-derived genomic DNA, we first screened all coding exons in which mutations have been reported previously.[4,5] Initially, we analyzed a total of 36 of 174 exons (*KDM3B* (2/24), *KDM5C* (9/26), *UTX* (7/29), *MLL2* (8/54), *EZH2* (1/20) and *SETD2* (9/21)) and found 7 non-synonymous tumor-specific aberrations. In AML, we found one *EZH2* mutation (p.G648E) in a t(8;21)-positive, and two *MLL2* missense mutations (p.R5153Q and p.Y5216S; Table 1) and one

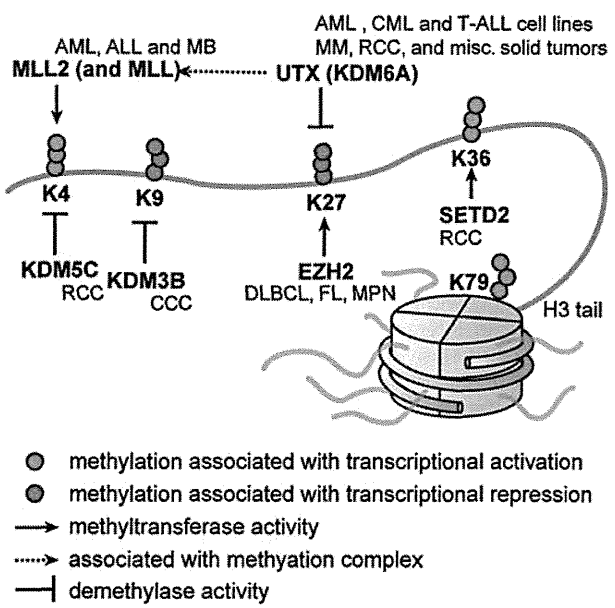

Figure 1. Histone 3 methylation and selected histone demethylases and methyltransferases. Cancers are shown in italics next to the mutated protein they are associated with. MM, multiple myeloma; FL, follicular lymphoma; DLBCL, diffuse large B-cell lymphoma; RCC, renal cell carcinoma; CCC clear cell carcinoma; MPN, myeloproliferative neoplasm; MB, medulloblastoma.

Accepted article preview online 1 March 2012; advance online publication, 3 April 2012

Chimeric antisense RNA derived from chromosomal translocation modulates target gene expression

Chromosomal translocations in hematologic malignancies[1] are closely related to the molecular pathogenesis. Usually, the directions of the two genes involved in the chromosomal translocations are the same, resulting in chimeric proteins that retain their functional domains. Here we report a chromosomal translocation from a myelodysplastic syndrome (MDS) patient resulting in a fusion gene consisting of the sense strand of the *TEL/ETV6* gene on 12p13 fused with the antisense strand of the Thousand-and-one amino acid protein kinase 1 (*TAOK1*) gene on 17q11. We suggest the possibility that the chimeric transcript may act as an antisense RNA on wild-type *TAOK1* mRNA, resulting in downregulation of *TAOK1* protein expression.

A 73-year old man was admitted to our hospital because of severe anemia (hemoglobin 5.5 g/dL) and thrombocytopenia (platelets 72×10^9/L). Bone marrow aspiration indicated dysplasia in three lineages with 11% blasts. The patient was diagnosed with MDS-RAEB-II. Chromosomal analysis of bone marrow cells revealed t(12;17)(p13;q11). Four months after diagnosis, disease progression to acute myelogenous leukemia was confirmed without additional chromosomal abnormalities. Conventional chemotherapy was performed, but he died of leukemia progression nine months after diagnosis.

Using leukemia cells at diagnosis, fluorescent *in situ* hybridization (FISH) analysis showed a split signal of *TEL/ETV6* gene (Figure 1A and B). The *TEL/ETV6* fusion transcript was amplified by 3′-RACE[2] and analyzed with DNA sequencing (*Online Supplementary Appendix*). The 3′ end of the exon 2 of *TEL/ETV6* was fused with antisense sequences of intron 19 of *TAOK1*, which was followed by antisense sequences of exon 19 and intron 18 of *TAOK1* (Figure 1C) (GenBank #JN603181). Amino acid sequences of the carboxyl (C)-terminus of exon 2 of TEL/ETV6 were followed by nonsense sequences derived from the antisense *TAOK1* sequences of intron 19 (Figure 1C and D).

Expression of the fusion transcript (*TEL-TAOK1ap*) was checked in primary bone marrow cells from MDS patients and cell lines by RT-PCR (TT-U and TT-L primers in Figure 1D), and showed that only the patient's sample that held t(12;17) expressed the *TEL-TAOK1ap* transcript (Figure 2A, lane 1). Expression of the wild-type (WT) TAOK1 protein was confirmed with immunoblotting using whole-cell lysates from cell lines and primary bone marrow cells from MDS patients (Figure 2B), indicating that the level of WT-TAOK1 protein expression was much lower in the patient's cells that held t(12;17) (lane 8) than in normal bone marrow cells (lane 1) and several leukemia cell lines (lanes 2-7). Samples from other MDS patients (lanes 9-13) were analyzed; some patients also showed lower expression of WT-TAOK1 protein (lanes 9 and 10). Expression levels of *TAOK1* mRNAs were confirmed with quantitative (real-time) RT-PCR using the 3′ and 5′ region-specific probe sets for *WT-TAOK1* transcripts (Figure 2C). Expression of 5′- and 3′-*TAOK1* was lower in the t(12;17) patient's cells than in leukemia cell lines (Figure 2D). The expression levels of 5′ and the 3′ *TEL/ETV6* mRNAs were mostly similar in the patient's cells in semi-quantitative RT-PCR analysis (*data not shown*). These data suggest that WT-TAOK1 protein expression is down-regulated in some MDS cases by unknown molecular mechanisms.

Next, we hypothesized that the antiparallel portion of exon 19 of *TAOK1* in *TEL-TAOK1ap* transcript may act as an antisense RNA to knock-down *WT-TAOK1* mRNA expression. To test this hypothesis, the *TEL-TAOK1ap* transcript was over-expressed in 293T cells. As a control, shRNA for *TAOK1* mRNA was transfected into 293T cells, resulting in a significant reduction in endogenous TAOK1 protein (Figure 2E). When using the *TEL-TAOK1ap* expression vector in 293T cells, endogenous TAOK1 protein expression was reduced in a dose-depen-

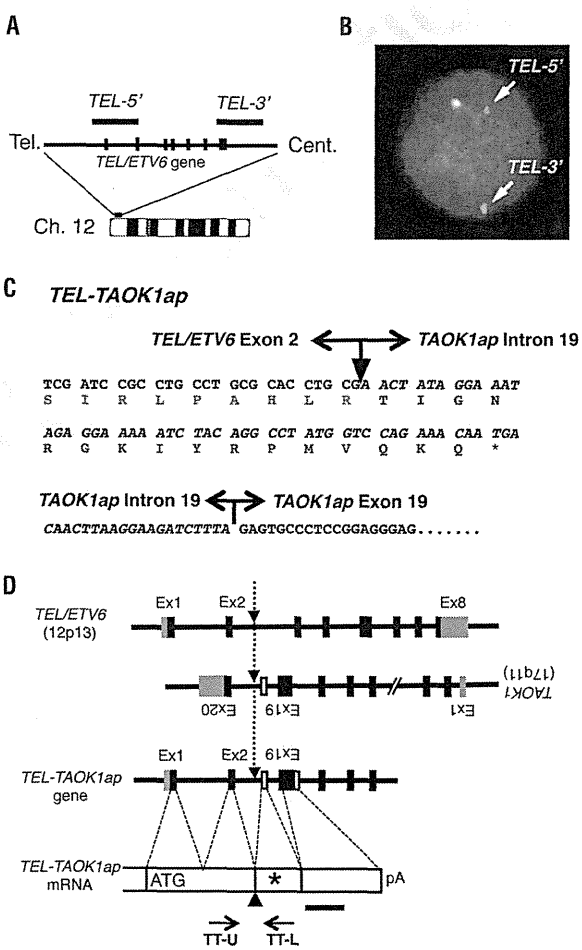

Figure 1. Aberrant fusion transcript derived from chromosomal translocation t(12;17)(p13;q11). (A) FISH probes for *TEL/ETV6*. (B) A split signal was observed in the patient's leukemia cells. Red signal is from the TEL-5′ probe, and green signal is from the *TEL-3′* probe. Non-split signal from wild-type *TEL/ETV6* is observed as a yellow dot. (C) DNA sequence of the chimeric transcript (TEL-TAOK1ap) is shown in black letters. Amino acid sequence from exon 2 of TEL/ETV6 is indicated in red letters. Amino acid sequence from the antiparallel sequence of intron 19 of *TAOK1* is indicated in blue letters. Note that amino acid sequence in blue letters is completely different from the sequence of WT-TAOK1 protein. (D) Schematic representation of genomic structure around the breakpoint. Tel: telomere; cent: centromere; ap: antiparallel sequence; Ex; exon, *: stop codon; pA: poly adenine tail, black boxes; exons, shaded boxes; untranslated exon, white boxes; intron sequences that are utilized as exons in *TEL-TAOK1ap*.

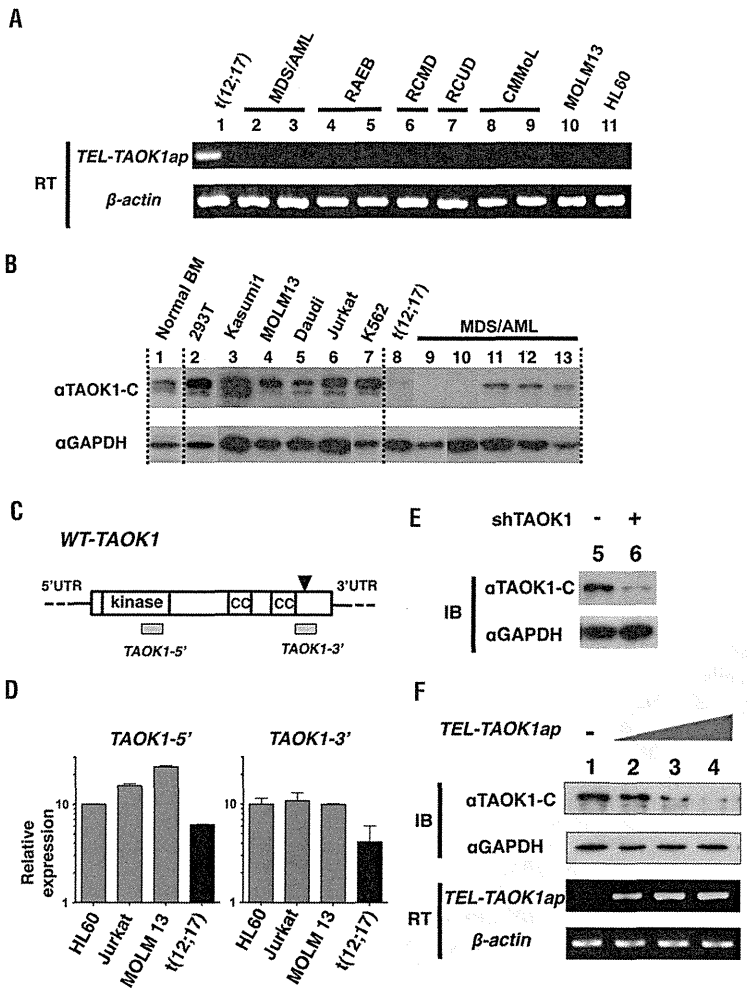

Figure 2. Expression of *TEL-TAOK1ap* chimeric transcript and its RNA interfering effect in regulating endogenous TAOK1 expression. (A) *TEL-TAOK1ap* transcript and (B) WT-TAOK1 protein expression in the patient's primary cells and human leukemia cell lines. RT-PCR (RT) (A) and immunoblotting (IB) using an anti-TAOK1-C-terminus antibody (B) were performed. The patient's samples holding t(12;17)(p13;q11) are indicated as t(12;17). Primary patient's bone marrow cells were used in lanes 1 to 9 in (A) and lanes 8 to 13 in (B). Beta-actin and GAPDH are the positive controls for RT-PCR and immunoblotting, respectively. (C) Schematic representation of *WT-TAOK1* mRNA. Shaded boxes indicate probes for quantitative RT-PCR. Black triangles indicate break point in the *TEL-TAOK1ap* fusion. (D) Quantitative RT-PCR using TAOK1-specific probes as indicated in (C). (E) Expression vector for shRNA against *TAOK1* mRNA or control mock vector (3 mg each) was transfected into 293T cells (5×10^5 cells). Immunoblotting for endogenous TAOK1 was performed using anti-TAOK1 C-terminus antibody. (F) Expression vector for *TEL-TAOK1ap* (0, 0.5, 1, and 3 μg in each sample) or the control mock vector (3, 2.5, 2, and 0 μg in each sample) was transfected into 293T cells (5×10^5 cells). Endogenous TAOK1 protein expression (upper panel) and over-expressed TEL-TAOK1ap transcript (third panel) were confirmed by IB and RT. Note that the endogenous TAO1 protein expression level was decreased in a dose-dependent manner. MDS/AML; acute myelogenous leukemia followed by MDS; RAEB: refractory anemia with excess blasts; RCMD: refractory cytopenia with multilineage dysplasia; RCUD: refractory cytopenia with unilineage dysplasia; CMMoL: chronic myelomonocytic leukemia; UTR: untranslated region; CC: coiled-coil domain.

dent manner (Figure 2F). These findings support our hypothesis that *TEL-TAOK1ap* has an RNA-interfering effect on *WT-TAOK1* mRNA.

A previous report showed that translocation of t(12;17)(p13;p12-p13) in secondary AML results in fusion of *TEL/ETV6* and the antisense strand of *PER1*.[3] Expression of the chimeric transcript containing antisense sequences to *PER1* was confirmed in this case. Recently, RNA interfering activity by small non-coding RNAs, such as small interfering RNA, micro-RNA, and PIWI-RNA,[4] has been reported. Furthermore, several reports have indicated that long non-coding RNAs[5] and natural antisense transcripts[6] play crucial roles in regulating mRNA expression of target genes. Our findings suggest a mechanism in which a chimeric transcript regulates target gene expression via an RNA interfering effect.

The *TEL-TAOK1ap* chimeric transcript may have dual functions, including an antisense effect to interfere with *WT-TAOK1* mRNA and production of C-terminally-truncated TEL/ETV6. A previous report indicated that TAOK1 is a serine/threonine kinase that plays an important role in the p38 MAPK signaling pathway.[7] Knockdown of TAOK1 in HeLa cells disrupts normal cell division due to a disorder in the spindle checkpoint function.[8] In our experiment (Figure 2B), some MDS patients showed relatively lower expression of WT-TAOK1 protein compared with acute leukemia cell lines, suggesting that lower expression might be related to the pathogenesis of MDS, such as aberrant cell division and/or dysplasia. Furthermore, there are many reports of TEL/ETV6 fusion proteins that contain the N-terminus of TEL/ETV6 in leukemia patients,[9] suggesting that aberrant substitution or truncation of the C-terminus of TEL/ETV6 may contribute to leukemia biology. The biological significances of *TEL-TAOK1ap* chimeric transcripts and their relationship with MDS/leukemia genesis require further study.

Takumi Sugimoto,[1,2] Akihiro Tomita,[1] Akihiro Abe,[1,3] Chisako Iriyama,[1] Hitoshi Kiyoi,[1] and Tomoki Naoe[1]*

[1]Department of Hematology and Oncology, Nagoya University Graduate School of Medicine, Nagoya, Aichi, Japan; [2]Department of Hematology and Oncology, Toyohashi Municipal Hospital, Toyohashi, Aichi, Japan; and [3]Department of Hematology, Fujita Health University School of Medicine, Toyoake, Aichi, Japan

Correspondence: Akihiro Tomita, Department of Hematology and

Oncology, Nagoya University Graduate School of Medicine, Tsurumai-cho 65, Showa-ku, Nagoya 466-8550, Japan. Phone: international +81.52.7442145. Fax: international +81.52.7442161. E-mail: atomita@med.nagoya-u.ac.jp

The online version of this article has a Supplementary Appendix.

Key words: chimeric transcript, antisense RNA, TAOK1, myelodysplastic syndrome.

Citation: Sugimoto T, Tomita A, Abe A, Iriyama C, Kiyoi H, and Naoe T. Chimeric antisense RNA derived from chromosomal translocation modulates target gene expression. Haematologica 2012;97(8)1278-1280. doi:10.3324/haematol.2011.057869

Funding: this work was supported by Grants-in-Aid from the Ministry of Scientific Research of Education, Culture, Sports, Science and Technology, and the Ministry of Health, Labor and Welfare, and the Japanese Society for the Promotion of Science (117100000439). We are indebted to Chika Wakamatsu, Eriko Ushida, Mari Otsuka, and Yukie Konishi for their valuable assistance in the laboratory.

The information provided by the authors about contributions from persons listed as authors and in acknowledgments is available with the full text of this paper at www.haematologica.org.

Financial and other disclosures provided by the authors using the ICMJE (www.icmje.org) Uniform Format for Disclosure of Competing Interests are also available at www.haematologica.org.

References

1. Look AT. Oncogenic transcription factors in the human acute leukemias. Science. 1997;278(5340):1059-64.
2. Kuno Y, Abe A, Emi N, Iida M, Yokozawa T, Towatari M, et al. Constitutive kinase activation of the TEL-Syk fusion gene in myelodysplastic syndrome with t(9;12)(q22;p12). Blood. 2001;97(4): 1050-5.
3. Murga Penas EM, Cools J, Algenstaedt P, Hinz K, Seeger D, Schafhausen P, et al. A novel cryptic translocation t(12;17)(p13;p12-p13) in a secondary acute myeloid leukemia results in a fusion of the ETV6 gene and the antisense strand of the PER1 gene. Genes Chromosomes Cancer. 2003;37(1):79-83.
4. Moazed D. Small RNAs in transcriptional gene silencing and genome defence. Nature. 2009;457(7228):413-20.
5. Orom UA, Derrien T, Beringer M, Gumireddy K, Gardini A, Bussotti G, et al. Long noncoding RNAs with enhancer-like function in human cells. Cell. 2010;143(1):46-58.
6. Faghihi MA, Wahlestedt C. Regulatory roles of natural antisense transcripts. Nat Rev Mol Cell Biol. 2009;10(9):637-43.
7. Raman M, Earnest S, Zhang K, Zhao Y, Cobb MH. TAO kinases mediate activation of p38 in response to DNA damage. EMBO J. 2007;26(8):2005-14.
8. Draviam VM, Stegmeier F, Nalepa G, Sowa ME, Chen J, Liang A, et al. A functional genomic screen identifies a role for TAO1 kinase in spindle-checkpoint signalling. Nat Cell Biol. 2007;9(5):556-64.
9. Bohlander SK. ETV6: a versatile player in leukemogenesis. Semin Cancer Biol. 2005;15(3):162-74.

ELSEVIER

Experimental Hematology

Experimental Hematology 2012;40:724–737

CML cells expressing the TEL/MDS1/EVI1 fusion are resistant to imatinib-induced apoptosis through inhibition of BAD, but are resensitized with ABT-737

Kazuyuki Shimada[a,b,c], Akihiro Tomita[b], Yosuke Minami[b], Akihiro Abe[b,d], Charlotte K. Hind[c], Hitoshi Kiyoi[b], Mark S. Cragg[c], and Tomoki Naoe[b]

[a]*Institute for Advanced Research, Nagoya University, Nagoya, Japan;* [b]*Department of Hematology and Oncology, Nagoya University Graduate School of Medicine, Nagoya, Japan;* [c]*Antibody and Vaccine Group, Cancer Sciences Unit, Faculty of Medicine, University of Southampton, Southampton General Hospital, Southampton, UK;* [d]*Department of Hematology, Fujita Health University School of Medicine, Toyoake, Aichi, Japan*

(Received 26 January 2012; revised 2 May 2012; accepted 19 May 2012)

Chronic myeloid leukemia is the first disease in which the potential of molecular targeted therapy with tyrosine kinase inhibitors (TKIs) was realized. Despite this success, a proportion of patients, particularly with advanced disease, are, or become, resistant to this treatment. Overcoming resistance and uncovering the underlying mechanisms is vital for further improvement of clinical outcomes. Here we report the identification, development, and characterization of a novel chronic myeloid leukemia cell line carrying the additional chromosomal aberration t(3;12)(q26;p13) resulting in expression of the TEL/MDS1/EVI1 fusion protein, which is resistant to TKIs. Resistance to TKIs was overcome by the co-administration of the BH3-mimetic, ABT-737. In addition, application of EVI1-specific small interfering RNA decreased expression of the TEL/MDS1/EVI1 fusion, reduced resistance to imatinib, and increased sensitivity to ABT-737. Subsequent studies revealed a role for the BH3-only protein BAD, probably via a phosphoinositide 3-kinase/AKT-dependent pathway, as pharmacological inhibition of AKT could also resensitize cells to death from TKIs. These findings indicate a novel pathway of TKI resistance regulated by EVI1 proteins and provide a promising means for overcoming resistance in chronic myeloid leukemia and other hematological malignancies displaying EVI1 overexpression.

Chronic myeloid leukemia (CML) is characterized by the presence of the *BCR-ABL* fusion gene. Its powerful transforming potential results in cells with a strong proliferation advantage, which are refractive to apoptosis and independent of extracellular survival signals [1–3]. However, development of BCR-ABL inhibitors, imatinib, dasatinib, and nilotinib has revealed the Achilles heel aspect of this potent oncogenic kinase and has heralded in an era of targeted therapy [4–6]. These drugs eliminate signaling downstream of BCR-ABL and result in profound growth arrest and apoptosis. The resulting clinical efficacy of TKI in CML has lead to them replacing interferon-α as first-line therapy. However, although clinical efficacy is generally excellent in early-stage CML, once the disease has progressed from benign chronic phase into an accelerated phase or blast crisis, i.e., advanced disease, the clinical outcome is generally poor [4,7,8]. Thus, preventing disease progression and stabilizing the disease in chronic phase have been the guiding principles of CML treatment to date.

The mechanism of TKI resistance observed in a proportion of patients can be either BCR-ABL–dependent or –independent [9]. BCR-ABL–dependent mechanisms are characterized by the emergence of mutations in the tyrosine kinase domain, including the T315I mutation, and/or overexpression of the BCR-ABL protein due to gene amplification [10]. BCR-ABL–independent mechanisms are characterized by dysregulations in drug transport [11,12], protection in

Drs. Cragg and Naoe contributed equally to this study and are the joint senior authors.

Offprint requests to: Kazuyuki Shimada, M.D., Ph.D., Institute for Advanced Research/Graduate School of Medicine, Department of Hematology and Oncology, Nagoya University Graduate School of Medicine, 65 Tsurumai-cho, Showa-ku, Nagoya 466-8550, Japan; E-mail: kshimada@med.nagoya-u.ac.jp

Supplementary data related to this article can be found online at http://dx.doi.org/10.1016/j.exphem.2012.05.007.

0301-472X/$ - see front matter.
http://dx.doi.org/10.1016/j.exphem.2012.05.007

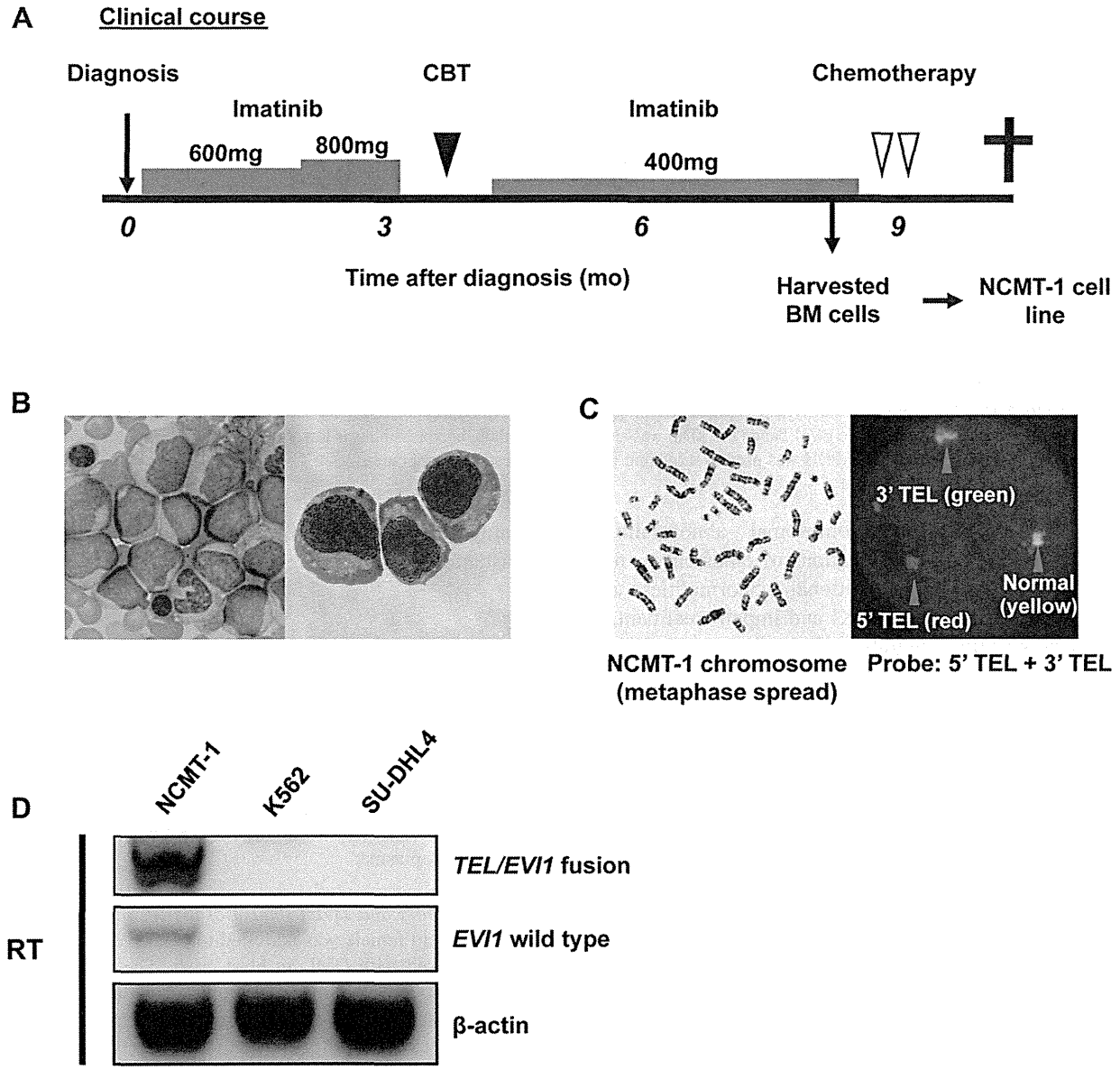

Figure 1. Clinical course of a patient with CML who was resistant to imatinib and molecular characterization of the NCMT-1 cell line. (**A**) A 36-year-old female was admitted to the affiliated hospital of Nagoya University in September 2005 and diagnosed with CML in blast crisis. The flow cytometric analysis revealed CD13, CD33, CD34, and HLA-DR positivity on her tumor cells. A 600-mg dose of imatinib was administered as the first line of therapy. Failure to obtain a full hematologic response resulted in a dose escalation to 800 mg during this first course of treatment. A complete hematological response was finally achieved, however, no cytogenetic response and no major molecular response were observed. Subsequently, 3 months after diagnosis, the patient received a cord blood stem cell transplant (CBT) (black triangle), but the bone marrow at the recovery phase of the transplant still included tumor cells. Imatinib was administered again after CBT, but her condition continued to deteriorate even during treatment. Finally, she received palliative chemotherapy (white triangle) and died of her disease in June 2006. (**B**) Bone marrow aspirate smear from a diagnostic sample from the patient (left panel) or cytospin specimens of NCMT-1 cells (right panel) stained with May-Grünwald-Giemsa staining and examined microscopically. Blast cells with Azur granules are clearly seen in the specimens. (**C**) Chromosomal analysis of the NCMT-1 cell line revealed a complicated karyotype, including 3q26 abnormalities and t(9;22)(q34;q11.2) in G-banding analysis (left panel), and a split signal of the 5′ and 3′ *TEL* gene probes in fluorescence in situ hybridization analysis (right panel), indicating maintenance of the t(3;12)(q26;p13) translocations in the NCMT-1 cells. (**D**) Reverse transcriptase (RT) PCR analysis of NCMT-1, K562, and SU-DHL4 cells. Complementary DNA from each cell line was prepared and then subjected to PCR using primers to *TEL* and *EVI1* to detect the fusion gene or *EVI1* alone to detect the wild-type product. A single band indicating the *TEL/EVI1* fusion was detected in NCMT-1, but not K562 or SU-DHL4 cells. Using EVI1-U and EVI-L primers, the *EVI1* wild-type band was also detected in NCMT-1 and K562 cells. A PCR reaction using primers for β-actin was also performed as an inter-sample and loading control.

the bone marrow niche, activation of other oncogenes (e.g., LYN) [13,14], or tumor dormancy [15,16]. Treatment in each case becomes far more difficult, and so uncovering means of overcoming resistance is vital.

During disease development and in chronic phase, the initiating lesion BCR-ABL is thought to cause genetic instability, resulting in additional genetic abnormalities in genes associated with proliferation, differentiation, and

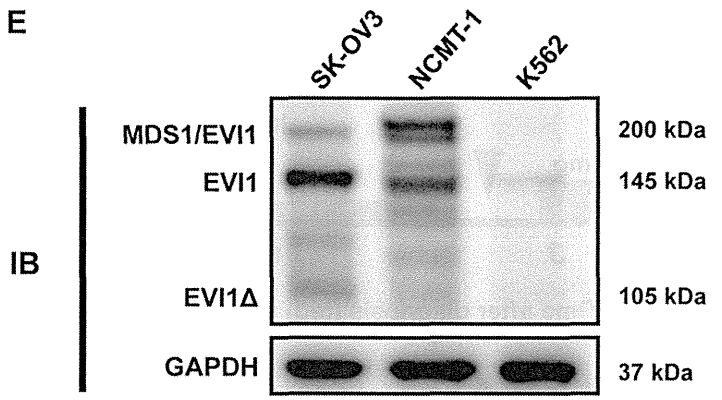

Figure 1. (*Continued*) (**E**) Immunoblotting (IB) analysis of NCMT-1 and K562 cells. Whole cell lysates were prepared from each cell line and assessed by immunoblotting for MDS1/EVI1 or glyceraldehyde phosphate dehydrogenase (GAPDH). Expression of the fusion protein (200 kDa) was strongly detected in NCMT-1 but not K562 cells. The wild-type EVI1 band (145 kDa) was also detected although expression was lower than the fusion protein. SK-OV3 was used as a positive control of EVI1 protein. GAPDH was used as a loading control on the same membrane.

apoptosis [1]. Typically, chromosomal abnormalities including trisomy 8 and translocations of other oncogenes are acquired [17]. These additional abnormalities are thought to cause resistance to TKI and impair treatment.

EVI1 (ectopic viral integration site 1) is a transcription factor with two zinc finger motifs, and its acquisition is known to be a poor prognostic factor for acute myeloid leukemia [18]. *EVI1* is located on 3q26, and aberrant expression is mainly mediated by the t(3;3)(q21;q26), inv(3)(q21q26), t(3;12)(q26;p13), and t(3;21)(q26;q22) genomic aberrations [19–21]. The t(3;12)(q26;p13) resulting in the *TEL/MDS1/EVI1* fusion is reported in CML, acute myeloid leukemia, and myelodysplastic syndrome [22]. EVI1 itself is indispensable for proliferation of hematopoietic stem cells [23] and possesses various oncogenic functions, including suppression of transforming growth factor–β [24], negative regulation of the c-Jun N-terminal kinase pathway [25], and stimulation of cell growth by *AP-1* [26]. However, its impact on apoptotic regulation has not been well studied.

Here we report on the establishment of a novel CML cell line derived from a patient who developed CML in blast crisis and was refractory to various treatments, including TKI and stem cell transplantation. The tumor at diagnosis indicated t(3;12)(q26;p13) as an additional chromosomal abnormality, and this was retained in the established cell line. The cell line also retained resistance to TKI, providing us with a valuable tool for understanding the mechanism of TKI resistance and allowing us to investigate the contribution of the t(3;12)(q26;p13) in this. Using *EVI1*-specific small interfering RNA (siRNA), we were able to reduce expression of the fusion protein and show that resistance was due, at least in part, to the inhibition of BAD by AKT downstream of EVI1 signaling. We were also able to show that TKI resistance could be overcome by addition of the BH3-mimetic, ABT-737, or an AKT inhibitor, indicating two separate approaches that might offer better treatment strategies for EVI1-overexpressing leukemias resistant to TKI.

Material and methods

Chemicals, reagents, and cell lines

Imatinib was supplied by Novartis (Basel, Switzerland). Dasatinib was supplied by Bristol-Myers Squibb (New York, NY, USA). AKT inhibitor VIII was purchased from Merck (Nottingham, UK). K562 were obtained from the ATCC (Manassas, VA, USA). All cultures were monitored routinely and found to be free of mycoplasma.

Clinical history and establishment of the NCMT-1 cell line

A 36-year-old female was admitted to Ogaki Municipal Hospital and diagnosed with CML in blast crisis. She was administered imatinib (600 mg) immediately following diagnosis and then a higher dose (800 mg) during treatment to achieve a hematological response, but a full cytogenetic response was not observed. A <1-log reduction of tumor was observed by quantitative polymerase chain reaction (PCR) [27]. Following the failure of imatinib, the patient received a cord blood stem cell transplant, but this did not arrest the disease. Subsequently, imatinib was readministered, but it again failed to fully control the disease and the patient died 9 months after diagnosis. Bone marrow cells obtained at the refractory phase after transplantation were subsequently used to establish a cell line. Mononuclear cells were purified with Ficoll-Conray solution and cultured in Iscove's modified Dulbecco's medium (Sigma Aldrich, St Louis, MO, USA) supplemented with 20% fetal calf serum. The medium was changed every 1 to 2 weeks. After observing prolonged growth, the cell line (termed *NCMT-1*) was considered established and the fetal calf serum concentration reduced to 10%.

Cytogenetic analysis

Chromosomal G-banding was performed by the Mitsubishi Chemical Medience Corporation (Tokyo, Japan). TEL gene translocation was analyzed by fluorescence in situ hybridization by SRL, Inc. (Tokyo, Japan).

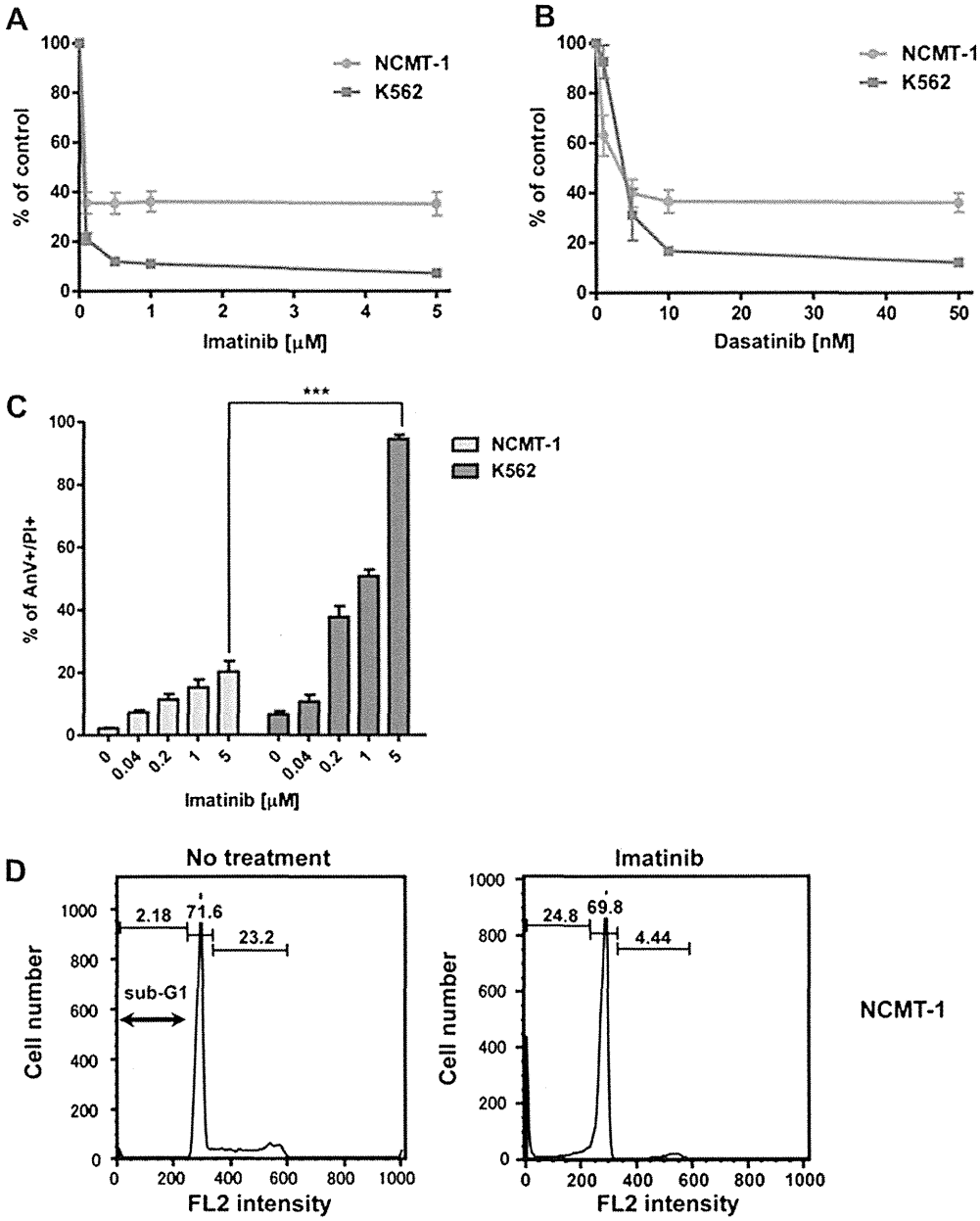

Figure 2. NCMT-1 cells have partial resistance to TKI. (**A**, **B**) To evaluate cell proliferation in the presence of various concentrations of TKI, the MTT assay was performed on K562 or NCMT-1 cells after 72 h of incubation in the presence of imatinib (0.1, 0.5, 1, and 5 μM) (**A**), or dasatinib (1, 5, 10, and 50 nM) (**B**). Inhibition of cell proliferation in NCMT-1 cells (gray circles) is clearly less than that observed with K562 cells (black squares) with both TKIs. Each point represents the mean value taken from three independent experiments, with error bars indicating the standard error of the mean (SEM). (**C**) Death assay in NCMT-1 and K562 cells after imatinib treatment. After 48-h incubation in the presence of various concentrations of imatinib (0, 0.04, 0.2, 1, and 5 μM), Annexin V (AnV)-FITC/PI cell death assays were performed. The amount of cell death induced in NCMT-1 cells was clearly less than induced in K562 cells ($p < 0.0001$ at 5 μM). Each point represents the mean value taken from three independent experiments, with error bars indicating SEM. (**D**, **E**) Cell cycle analysis after imatinib treatment. NCMT-1 (**D**) and K562. (**E**) cells were treated with 0.5 μM imatinib for 72 h, then lysed in hypotonic PI solution and assessed by flow cytometry. In NCMT-1 cells, the transition from the G_1 to the S and G_2/M phase was clearly inhibited in the presence of imatinib, indicative of cell cycle arrest (**D**).

RNA preparation, reverse transcriptase PCR, and DNA sequence analysis

Total RNA was extracted from cells using PureLink RNA Mini Kit (Invitrogen, Carlsbad, CA, USA) according to manufacturer's protocol. Complementary DNA was prepared with SuperScript III reverse transcriptase and random primers (Invitrogen). To detect the *TEL/EVI1* fusion, the *EVI1* wild-type gene transcript and β-actin messenger RNA, the primers listed in Supplementary Table E1 (online only, available at www.exphem.org) were used. Reverse transcriptase PCR with GoTaq hot start polymerase (Promega, Southampton, UK) was performed as described previously [28]. Images obtained with the GelDocXR

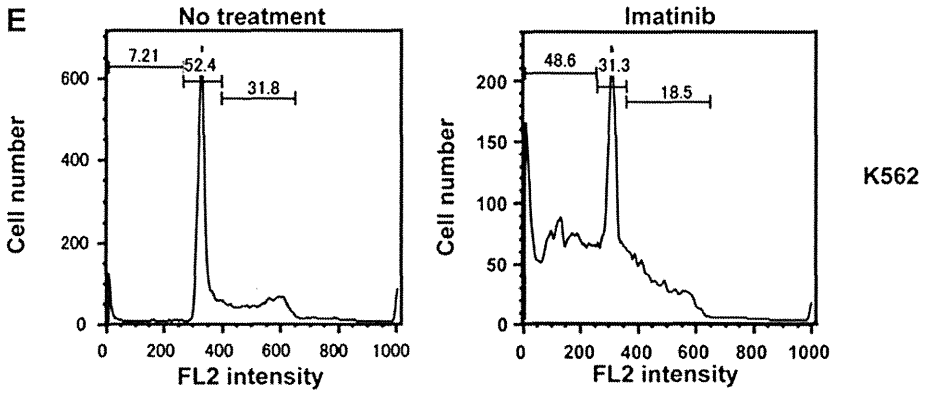

Figure 2. *(Continued)* In K562 (**E**) cells, the sub-G_1 population was far more evident compared to NCMT-1 cells.

imaging system (Bio-Rad, Hempstead, UK) were analyzed with Adobe Photoshop CS4 (Adobe Systems, San Jose, CA, USA). Sequencing was performed using the BigDye Terminator Cycle Sequencing Kit (Applied Biosystems, Foster City, CA, USA) and the product directly sequenced using an ABI 310 automated DNA sequencer (Applied Biosystems).

MTT assay

To evaluate cell proliferation, we performed MTT assays. Cells (2.5×10^4 for NCMT-1 and 1.0×10^4 for K562) were placed in 96-well plates and cultured for 72 h at 37°C in a 5% CO_2 incubator. Ten microliters TetraColor ONE (Seikagaku Biobusiness Corporation, Tokyo, Japan) was then added into each well and the fluorescence evaluated at 450 nM.

Cell death and cell cycle assessment

To evaluate cell death, the propidium iodide (PI) and Annexin V–fluorescein isothiocyanate (FITC) assay was performed as detailed previously [29]. Cells were placed in 96-well plates, incubated with the required drugs for 48 h, stained with 5 μg/mL PI and 1.6 μg/mL Annexin V-FITC for 15 min at room temperature in the dark, and cell death evaluated by flow cytometry (FACScan or FACSCalibur; BD, Franklin Lakes, NJ, USA). For cell cycle assessment, cells were assessed using the hypotonic PI assay detailed previously [30,31]. Cells were incubated for 72 h with imatinib, washed, and resuspended in phosphate-buffered saline containing 0.2% Triton X-100 and 50 μg/mL PI before analysis by flow cytometry as described.

Immunoblotting

Cells were treated as detailed and then lysed as described previously [32]. When required, 50 mM NaF and 1.68 mM Na_3VO_4 were added to prevent post-lysis changes in phosphorylation. After centrifugation (13,000 rpm for 10 min), sample buffer containing 5% 2-mercaptoethanol was added. After boiling for 5 min, samples were separated by sodium dodecyl sulfate polyacrylamide gel electrophoresis, transferred to polyvinyldene difluoride membranes and blocked with 5% skimmed milk in TBS-Tween buffer (50 mM Tris-HCl [pH 7.4], 150 mM NaCl and 0.05% Tween 20). Immunoblotting was carried out using primary antibodies (Supplementary Table E2; online only, available at www.exphem.org) appropriately diluted in TBS-Tween buffer with 5% bovine serum albumin and 0.05% sodium azide; horseradish peroxidase–conjugated secondary monoclonal antibodies (GE Healthcare, Chalfont St Giles, UK) were used as described and detected with Amersham ECL-plus (GE), Super-Signal West Pico (Thermo Scientific, Rockford, IL, USA) or Immobilon Western Substrate (Millipore, Billerica, MA, USA). Images obtained with the BioSpectrum AC system were analyzed with VisionWorksLS software (UVP, LLC, Cambridge, UK).

EVI1 knockdown

Transfection of siRNA (300 nM) was performed by Nucleofection using Amaxa Nucleofector Kit V (Lonza, Basel, Switzerland) according to manufacturer's protocol. siRNAs for *EVI1* were from Invitrogen (Stealth Select RNAi; Invitrogen) and control siRNA (Silencer Negative Control #1 siRNA) were from Applied Biosystems. Knock-down was confirmed by immunoblotting 48 h after transfection.

Statistical analysis

Statistical significance in the MTT and cell death assays was evaluated by unpaired *t* test using GraphPad PRISMv5 (GraphPad Software Inc. La Jolla, CA, USA). To calculate synergy, data was analyzed with CalcuSyn software (BIOSOFT, Cambridge, UK).

Results

Establishment of a CML cell line expressing the TEL/EVI1 fusion

During our routine clinical practice, we encountered a CML patient who was refractory to imatinib. The detailed clinical course of this patient and pathological specimens at her diagnosis are shown in Figure 1A, B. Given the unusual clinical course, we generated a cell line from the bone marrow cells obtained at the refractory phase ~8 months after diagnosis. A cell line, NCMT-1, developed (Fig. 1B, right panel). Chromosomal analysis revealed 46, XX, -1, der(1)?dup(1)(p13p22)inv(1)(p22q21)del(1)(q21q23), −2, add(3)(q26), add(6)(p23), t(9;22)(q34;q11.2), add(12)(p11.2), −20, +der(?)t(?;1)(?;q21), +2mar [20/20], indicating the continuing presence of the *EVI1* gene abnormality and *BCR-ABL* fusion in the clonal cell line (Fig. 1C, left panel).

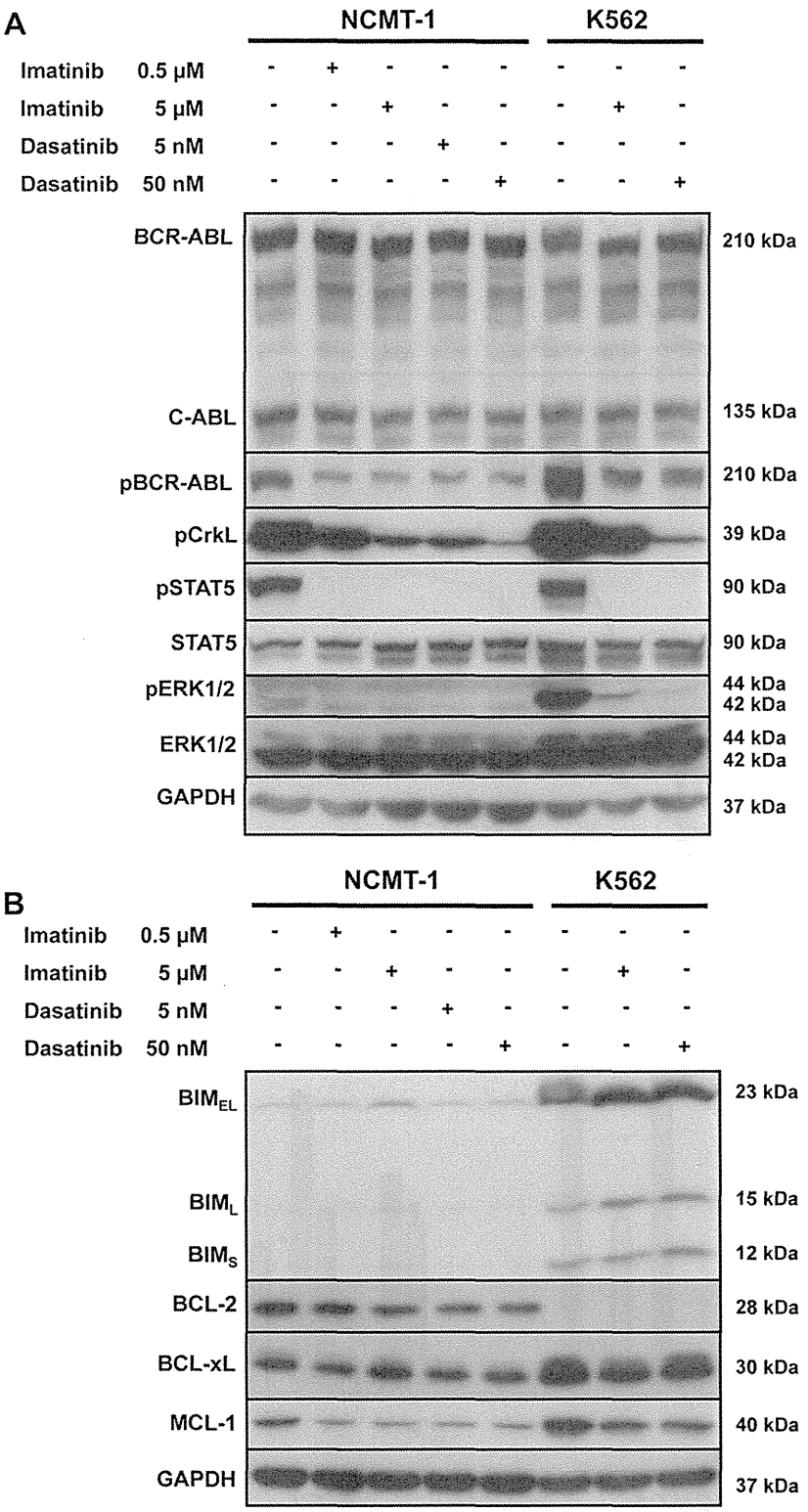

Figure 3. Immunoblotting analysis of NCMT-1 and K562 cells in the presence or absence of TKI. Whole cell lysates from each sample were obtained after 6-h incubation with TKI at the indicated dose, before analysis by immunoblotting. In both NCMT-1 cells, resistant to TKI, and K562 cells, sensitive to TKI, a similar signaling pathway downstream of BCR-ABL is in evidence, indicated by the dephosphorylation of BCR-ABL, CrkL, and signal transducers and activators of transcription (STAT) 5 after TKI treatment. (**A**) Analysis of signaling proteins: BCR-ABL, c-ABL, CrkL, STAT5, and glyceraldehyde phosphate dehydrogenase (GAPDH) as a loading control. (**B**) Analysis of apoptosis proteins: BIM, BCL-2, BCL-xL, MCL-1, and GAPDH as a loading control. BIM is less well expressed in NCMT-1 cells compared to K562 cells, and BCL-2 is expressed at high levels in NCMT-1 cells compared to K562 cells. All of the blotting was performed on membranes obtained from the same whole cell lysates.

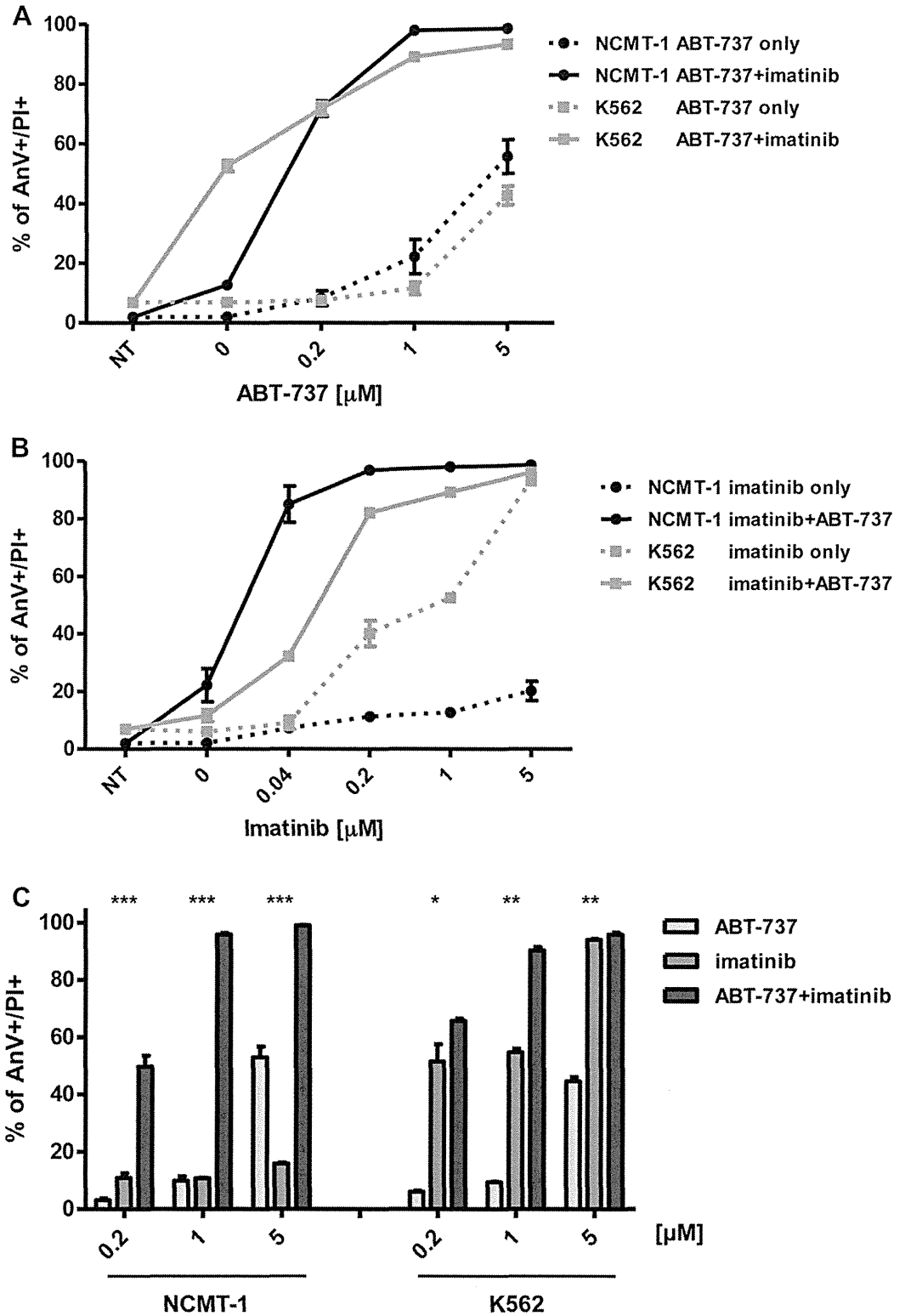

Figure 4. The resistance to TKI in NCMT-1 cells is overcome by the BH3-mimetic, ABT-737. NCMT-1 or K562 cells were treated with combinations of imatinib, ABT-737, or both for 48 h, before analysis of cell death using flow cytometric Annexin V-FITC/PI assays. (**A**) Cell death observed using various concentrations of ABT-737 with or without a constant dose of 1 μM imatinib. (**B**) Cell death observed using various concentrations of imatinib with or without a constant dose of 1 μM ABT-737. (**C**) Cell death observed using equal concentrations of imatinib and ABT-737 over a range of doses (0.2, 1, 5 μM). At each dose, the combination of imatinib and ABT-737 produced a significant synergistic effect in both cell lines. Synergistic effects were calculated by CalcuSyn software. Asterisks indicate the combination index (CI) of each dose as follows; $*5 \times 10^{-2}$–5×10^{-7}, $**5 \times 10^{-7}$–5×10^{-12}, $***<5 \times 10^{-12}$. Each point represents the mean value taken from three independent experiments with error bars indicating standard error of mean.

Table 1. Combination index

Cell line	Combination (μM)		Combination index
	Imatinib	ABT-737	
K562	0.2	0.2	0.004
	1	1	4.70E-07
	5	5	4.58E-09
NCMT-1	0.2	0.2	2.28E-12
	1	1	6.94E-27
	5	5	5.55E-33

To examine whether t(3;12) was maintained in the cell line, we performed fluorescence in situ hybridization analysis using 5′ (red) and 3′ (green) TEL probes. This analysis showed divided 5′ and 3′ probes indicating that the *TEL* translocation observed in the patient cells was maintained in the cell line (Fig. 1C, right panel).

Previous reports revealed that the *TEL/MDS1/EVI1* fusion gene was constructed from the fusion between Exon 2 of *TEL*, *MDS1*, and Exon 2 of *EVI1* as the break points [33]. To confirm the existence of the *TEL/EVI1* fusion in NCMT-1 cells, we performed reverse transcriptase PCR using *TEL*- and *EVI1*-specific primers. This analysis indicated high expression of the *TEL/EVI1* fusion in NCMT-1 (Fig. 1D, top panel), but not control (K562 or SU-DHL4) cells. Furthermore, reverse transcriptase PCR using *EVI1*-specific primers directed to the sequence upstream of the expected break point and to Exon 3 indicated weak expression of wild-type *EVI1* in NCMT-1 and K562 cells (Fig. 1D, middle panel). Sequencing of the amplified DNA confirmed the existence of the *TEL/MDS1/EVI1* fusion, with the expected break point (Supplementary Figure E1; online only, available at www.exphem.org). Protein expression of the fusion was confirmed by immunoblotting with high expression of the MDS1/EVI1 fusion observed, alongside correspondingly lower expression of the EVI1 protein, in NCMT-1 but not K562 cells (Fig. 1E).

Partial resistance of NCMT-1 cells to TKIs

As the CML from this patient was refractory to various treatments including imatinib, we performed the MTT assay to examine whether the cell line was resistant to the TKIs imatinib and dasatinib. This indicated that both TKIs potently suppressed proliferation of K562 cells, while only partially suppressing NCMT-1 proliferation. Accordingly, for imatinib, percent of control for NCMT-1 vs K562 was 7.2% vs 35.2% at 5 μM ($p = 0.004$); for dasatinib, percent of control was 12.2% vs 36.1% at 50 nM ($p = 0.004$) (Fig. 2A, B). Cell death evaluated by the Annexin V/PI assay revealed that NCMT-1 was significantly more resistant to imatinib compared to K562 (NCMT-1; 20.2%, K562; 94.5%, at 5 μM imatinib; $p < 0.0001$) (Fig. 2C). Cell cycle analysis after imatinib treatment revealed a clear population of sub-G_1, apoptotic cells in the K562 cell line, with very few sub-G_1 cells induced in the NCMT-1 cell line. However, profound G_1-arrest was observed in NCMT-1 cells, indicating that BCR-ABL is a key driver of proliferation for these cells and that they retain sensitive to inhibition by the drug, but that they possess an additional anti-apoptotic regulator compared to K562 cells (Fig. 2D, E).

Downstream signaling from BCR-ABL is correctly transduced in NCMT-1 cells

As detailed here, acquired resistance to imatinib can result from several sources. To determine the basis of resistance in NCMT-1 cells, we first analyzed the sequence of *BCR-ABL* in these cells and confirmed that no mutations were present in the gene (data not shown). To confirm that resistance was not due to overexpression of BCR-ABL, we performed immunoblotting and showed that the expression of BCR-ABL in resistant (NCMT-1) vs sensitive (K562) cells was equivalent (Fig. 3A, top panel).

Subsequently, to confirm whether the anticipated downstream intracellular signals from *BCR-ABL* were transduced in NCMT-1 cells and blocked by the TKI, we performed further immunoblotting. As shown in Figure 3A, phosphorylation of BCR-ABL was markedly reduced in the presence of imatinib and dasatinib in both K562 and NCMT-1 cells. Further markers of downstream signaling (phosphorylated CrkL and signal transducers and activators of transcription 5) were also suppressed in the presence of imatinib and dasatinib in NCMT-1 and K562 cells. Taken together, we conclude that the immediate downstream signaling from BCR-ABL is typical in NCMT-1 cells, and broadly similar to that seen in TKI-sensitive K562 cells. As the immediate downstream signaling was normal in NCMT-1 cells, we subsequently analyzed the apoptosis-related proteins in NCMT-1 and K562 cells before and after TKI treatment.

We previously demonstrated that the induction of apoptosis in CML cells after imatinib treatment is regulated by the members of the BCL-2 family and we examined the expression of these proteins [34]. In NCMT-1 cells, the pro-apoptotic BH3-only protein BIM was apparently suppressed and not strongly upregulated in the presence of imatinib or dasatinib, in contrast to K562 cells (Fig. 3B and [34]). Furthermore, the pro-survival protein, BCL-2 was strongly expressed in NCMT-1 cells and absent in K562 cells. The expression of other pro-survival proteins, including BCL-xL and MCL-1, were broadly similar in both NCMT-1 and K562 cells (Fig. 3B and data not shown).

ABT-737 resensitizes NCMT-1 cells to imatinib

ABT-737 is a BH3-mimetic that inhibits the function of a subset of the pro-survival proteins (BCL-2, BCL-xL, and BCL-w) and, as a single agent, can lead to apoptosis of tumor cells dependent on these pro-survival molecules [35]. Previous reports suggest that ABT-737 can play an important role in overcoming resistance to TKI [34], thus we analyzed the ability of ABT-737 to resensitize NCMT-1

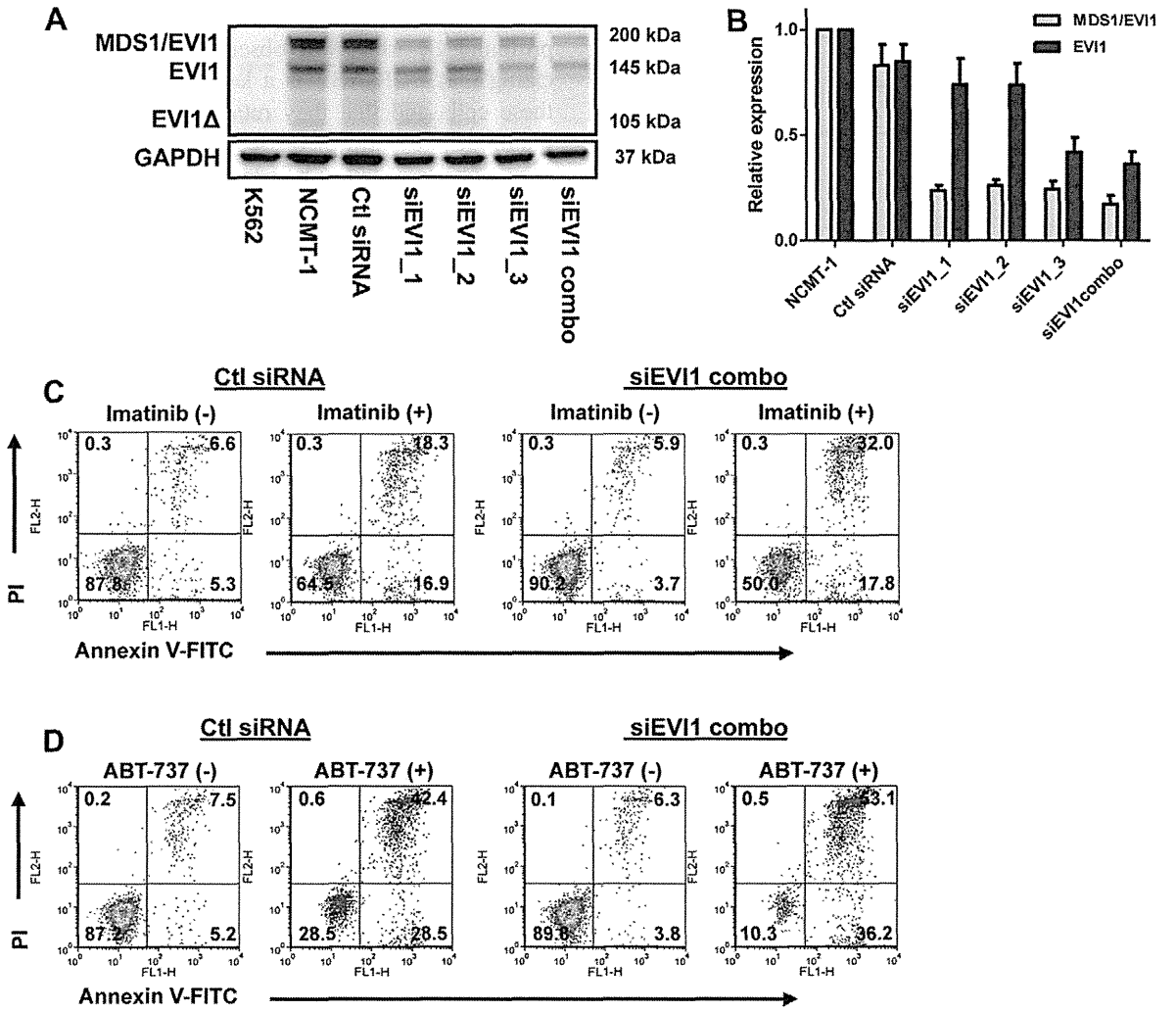

Figure 5. MDS1/EVI1 and EVI1 knockdown results in the suppression of phosphorylated-BAD via the AKT pathway, and partially restores the sensitivity to imatinib in NCMT-1 cells. (**A**) Whole cell lysates were obtained 48 h after nucleofection of NCMT-1 cells with the siRNA indicated. Immunoblotting for MDS1/EVI1 and glyceraldehyde phosphate dehydrogenase (GAPDH) as a loading control was then performed. (**B**) Densitometry analysis of MDS1/EVI1 and EVI1 expression normalized to GAPDH was performed. Each point represents of mean value taken from six independent experiments, with error bars indicating standard error of mean. (**C, D, E, F**) Sensitivity of siEVI1-transfected NCMT-1 cells to imatinib and ABT-737. NCMT-1 cells nucleofected with the siRNA indicated were rested for 48 h before addition of 5 μM imatinib (**C**) or 5 μM ABT-737 (**D**) for 48 h and assessment of cell death performed as in Figure 4. These data indicate the partial restoration of sensitivity to imatinib (**C**) and ABT-737 (**D**) in NCMT-1 cells transfected with siEVI1 compared to control siRNA.

cells to imatinib. In the presence of various concentrations of ABT-737 ± a constant dose of imatinib (1 μM), we performed cell death assays on NCMT-1 and K562 cells. In the presence of imatinib alone, we observed that NCMT-1 cells were resistant and K562 cells sensitive, as before. However, the cell death induced by imatinib was clearly increased in the presence of ABT-737 in both cell lines (Fig. 4A) with as little as 0.2 μM ABT-737, resulting in death of 70% to 80% of the cells. In the reciprocal experiment, varying the level of imatinib in the presence of a constant (1 μM) ABT-737, cell death was again clearly increased, especially in the NCMT-1 cells at extremely low doses (0.04 μM) of imatinib (Fig. 4B). To more formally evaluate the synergistic effect of imatinib combined with ABT-737, we analyzed cell death in the presence of equivalent concentrations of both drugs. As shown in Table 1, significant synergy, indicated by a combination index of <1, was observed at all three concentrations of drugs assessed (0.2, 1, and 5 μM) in NCMT-1 and K562 cells, however, the combination index was much lower, indicative of stronger synergy, in NCMT-1 rather than K562 cells (Fig. 4C). These data clearly indicate that ABT-737 can potently overcome the resistance of NCMT-1 cells to imatinib.

MDS1/EVI1 overexpression is associated with resistance to imatinib in NCMT-1 cells

To uncover whether the MDS1/EVI1 fusion was associated with the observed resistance to imatinib, we analyzed its

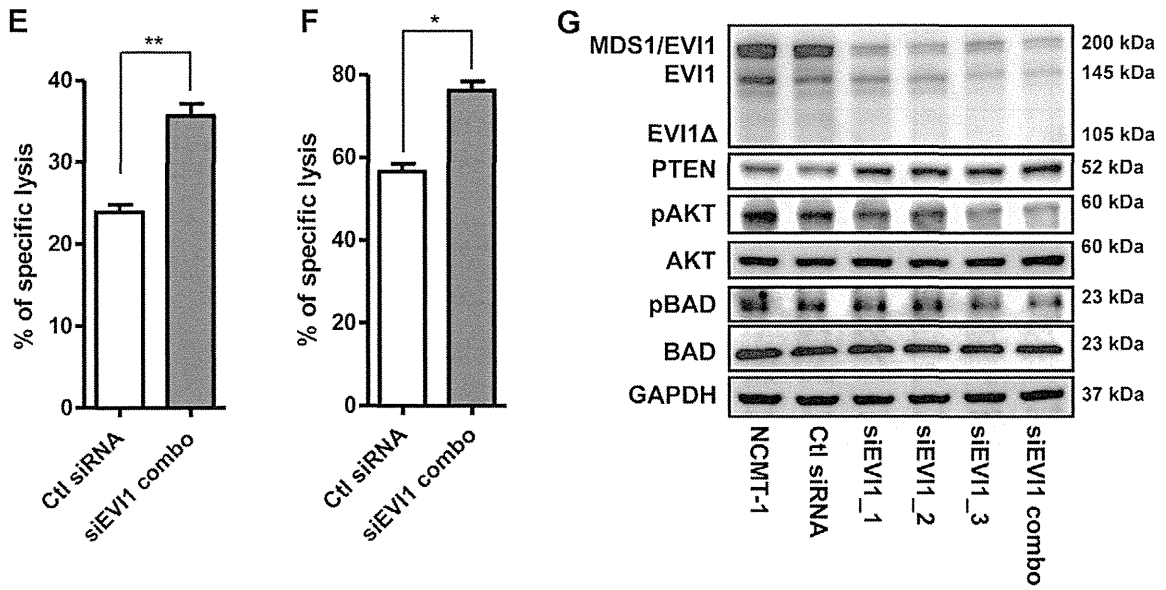

Figure 5. (*Continued*) Results are shown as representative dot plots from three to four independent experiments and are summarized in (**E**) and (**F**). Each point represents the mean value taken from two to three independent experiments, with error bars indicating the SEM. Asterisks indicate the p value as follows; *0.05, **0.005. (**G**) Whole cell lysates were obtained 48 h after nucleofection of NCMT-1 cells with the siRNA indicated. Immunoblotting for MDS1/EVI1, PTEN, AKT, pAKT, pBAD, BAD, and GAPDH as a loading control was then performed. Analysis of siEVI1-transfected NCMT-1 cells revealed the upregulation of PTEN and the downregulation of pAKT and pBAD (pSerine 136). All of the images except that relating to pBAD and BAD were derived from the same membrane. The pBAD and BAD blot was taken from a separate membrane using the same cell lysate.

role in NCMT-1 cells by reducing its expression using a panel of EVI1-specific siRNAs (siEVI1). Using three different siEVI1, alone and in combination (combo; where each was added in a one-third dose), we nucleofected NCMT-1 cells and confirmed the suppression of both the MDS1/EVI1 fusion and, to a lesser extent, the EVI1 protein by immunoblotting (Fig. 5A, B). We subsequently assessed the sensitivity of these cells to imatinib treatment. Cell death assays indicated that reduction in MDS1/EVI1 and EVI1 expression by the siEVI1 produced a partial but robust and statistically significant ($p = 0.003$) restoration of sensitivity to imatinib compared to the control siRNA-transfected NCMT-1 cells (Fig. 5C, E). Furthermore, the sensitivity to ABT-737 was increased in siEVI1-transfected cells compared to control siRNA-transfected cells ($p = 0.02$) (Fig. 5D, F). Taken together, these data indicate that overexpression of the MDS1/EVI1 fusion (and potentially the EVI1 protein) in NCMT-1 cells is associated with the resistance to imatinib and sensitivity to ABT-737 by suppressing apoptosis.

Concurrently, we analyzed whether the effect of siRNA might be related to changes in the BCL-2 family members. Given the relatively high expression of BCL-2 and low expression of BIM in NCMT-1 cells (in comparison to K562 cells), we first considered whether MDS1/EVI1 might regulate these proteins. However, in siEVI1-transfected NCMT-1 cells, both BIM and BCL-2 were unchanged (Supplementary Figure E2; online only, available at www.exphem.org), indicating that the MDS1/EVI1 fusion does not regulate these proteins. Moreover, the expression of BCL-xL and MCL-1 also remained unaffected by siEVI1 transfection (Supplementary Figure E2; online only, available at www.exphem.org). As a recent report revealed that EVI1 repressed PTEN expression and activated AKT [36], we analyzed the AKT pathway in the siEVI1-transfected NCMT-1 cells. In these cells, the level of PTEN was increased and that of phosphorylated AKT (pAKT) was clearly decreased compared to untreated cells or control-transfected cells, although the total level of AKT remained unchanged (Fig. 5G). To confirm this observation and also potentially reveal a direct pathway toward apoptotic regulation, we subsequently probed the phosphorylation status of the pro-apoptotic BH3-only protein BAD, a known substrate of AKT, using phosphospecific antibodies. As anticipated, the extent of phospho-BAD was suppressed in siEVI1-transfected NCMT-1 cells (Fig. 5G). Taken together, these data indicate that overexpression of MDS1/EVI1 is associated with resistance to imatinib (and dasatinib) through the inhibition of apoptosis via AKT and its downstream substrate BAD (Figs. 5G and 6D).

AKT as a potential therapeutic target for EVI1-expressing tumors

As pAKT is upregulated in NCMT-1 cells and suppressed by the downregulation of EVI1, we investigated whether AKT inhibition is a potential therapeutic target for EVI1-positive tumors. In the presence of 50 μM AKT inhibitor (AKTi) alone, very little cell death was observed. Similarly, when up to 25 μM AKTi was combined with low (0.2 μM) or

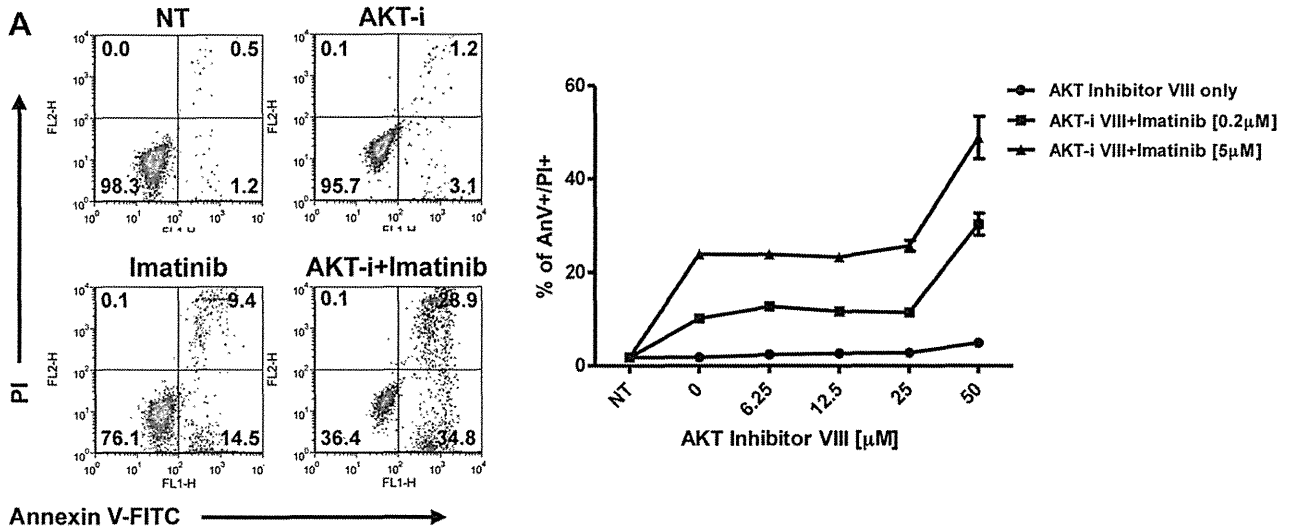

Figure 6. The resistance to TKI in NCMT-1 cells is overcome by the inhibition of AKT. NCMT-1 cells were treated with combinations of imatinib, AKT inhibitor (AKT-i), or both for 48 h, before analysis of cell death as in Figure 4. (**A**) Cell death observed using various concentrations of AKT-i with or without a constant dose of 0.2 or 5 μM imatinib. The representative dot plots of no treatment (NT), 5 μM imatinib alone, 50 μM AKT-i alone, and combination of these two were indicated. Each point represents the mean value taken from three independent experiments, with error bars indicating the standard error of mean (SEM).

high (5 μM) doses of imatinib, cell death was not increased compared to drugs alone. However, in the presence of 50 μM AKTi, cell death was clearly increased when combined with both high and low doses of imatinib (Fig. 6A). In the reverse experiment, varying doses of imatinib in the presence of a constant dose (50 μM) of AKTi, cell death was again increased in the presence of imatinib compared to imatinib alone (Fig. 6B). To confirm that these combination effects were specific for the inhibition of AKT, we investigated the phosphorylation status of AKT in the presence of varying doses of the AKTi. As expected, the phosphorylation status of AKT decreased substantially when the dose of inhibitor was increased from 25 μM to 50 μM, in keeping with the biological effects at these doses, but the total level of AKT remained unchanged (Fig. 6C). Further confirming the close association between the activation status of AKT and BAD, inhibition of pAKT correlated with a reduction in pBAD levels after treatment with the AKT inhibitor. Taken together, these data indicate that inhibition of pAKT resensitizes NCMT-1 cells to death with TKI. This effect mimics that seen following inactivation of EVI1, which indicates that targeting AKT could be a promising therapeutic strategy for treating EVI1-expressing tumors (Fig. 6D).

Discussion

Here, we have detailed the establishment of a novel, CML cell line, NCMT-1, which displays partial resistance to TKI, reflecting the clinical response of the patient from whom it was derived. Both the primary tumor and derived NCMT-1 cell line express the TEL/MDS1/EVI1 fusion protein derived from the t(3;12)(q26;p13) chromosomal abnormality. Our subsequent experiments revealed that overexpression of MDS1/EVI1 results in the inhibition of the pro-apoptotic protein, BAD, through effects on the AKT pathway. Addition of the BH3-mimetic, ABT-737, could overcome the resistance of the NCMT-1 cells to TKI and the combination of TKI + ABT-737 was highly synergistic in NCMT-1 as well as TKI-sensitive K562 cells. Finally, the combination of TKI + AKTi was also shown to resensitize NCMT-1 cells to apoptosis, indicating that AKT is a promising target for treating EVI1-positive malignancies.

Resistance to TKI in CML encompasses the BCR-ABL–dependent and –independent mechanisms detailed here [9]. In NCMT-1, no mutation of the BCR-ABL kinase domain was observed, and expression of BCR-ABL was shown by immunoblotting to be equivalent to that in the TKI-sensitive cell line K562. In addition, the immediate downstream signaling from BCR-ABL appeared similar to that seen in K562 cells, and sensitive to inhibition by imatinib, indicating a BCR-ABL–independent cause of resistance in NCMT-1 cells. The likely cause of the resistance in NCMT-1 is via an impact of MDS1/EVI1 on the BCL-2 family of apoptotic proteins. Furthermore, as ABT-737 combined with TKI could overcome the observed resistance to TKI, this indicates that the resistance was due to a downstream regulator of apoptosis, likely related to one or more BCL-2 family members known to be regulated by ABT-737 [37].

The patient from whose CML cells the NCMT-1 cell line was developed, presented in blast crisis and possessed the relatively rare chromosomal abnormality, t(3;12)(q26;p13) [22]. We observed the existence of this chromosomal aberration and also a relatively high expression of BCL-2 in the NCMT-1 cells and hypothesized that they were related to

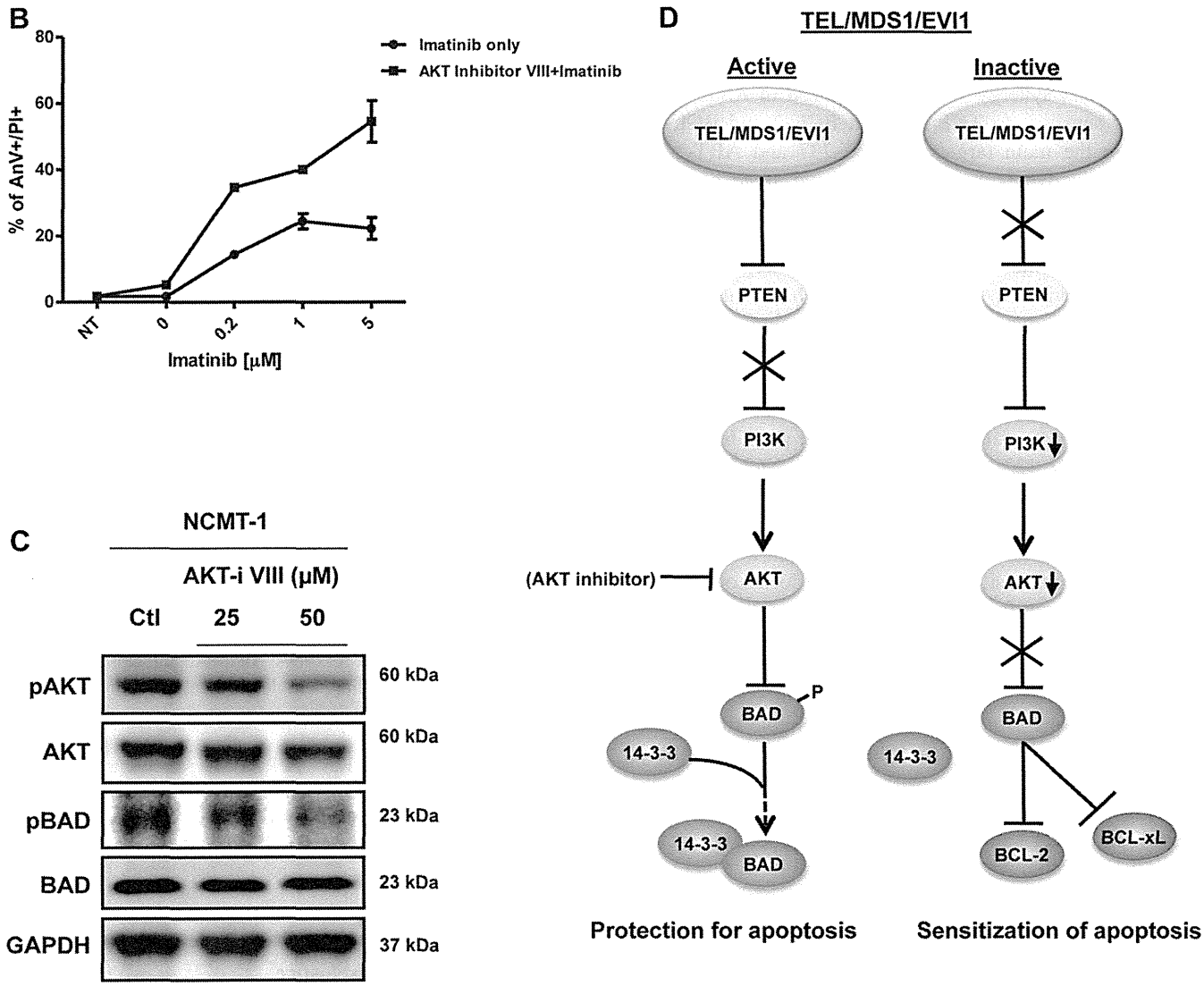

Figure 6. (*Continued*) (**B**) Cell death observed using various concentrations of imatinib with or without a constant dose of 50 μM AKT-i. Each point represents the mean value taken from three independent experiments, with error bars indicating the SEM. (**C**) Whole cell lysates were obtained 48 h after incubation with the AKT-i at various doses (0, 25, 50 μM). Immunoblotting for AKT, pAKT, BAD, pBAD, and glyceraldehyde phosphate dehydrogenase (GAPDH) as a loading control was then performed. (**D**) Schema representing the proposed downstream signaling pathway transduced by TEL/MDS1/EVI1. When TEL/MDS1/EVI1 is active, it suppresses PTEN resulting in activation of PI3K/AKT. Active, phosphorylated AKT leads to the phosphorylation of BAD, resulting in its binding to 14-3-3 protein, suppressing its pro-apoptotic activity. Conversely, when TEL/MDS1/EVI1 is not expressed or inactivated, PTEN suppresses the PI3K/AKT pathway. Reduced phosphorylation of BAD allows liberation from the 14-3-3 complex, augmenting its ability to counteract the protective functions of BCL-2 and BCL-xL, leading to sensitization of apoptosis. Inhibition of AKT mimics inactivation of EVI1.

disease progression in blast crisis. Using *EVI1*-specific siRNA, we were able to demonstrate that MDS1/EVI1 does not regulate BCL-2 (or BIM) expression in NCMT-1 cells, indicating an alternative mechanism. Previous reports suggest that overexpression of LYN can result in BCL-2 expression, however, in that report, LYN inhibited the immediate signaling pathway downstream of BCR-ABL, including effects on signal transducers and activators of transcription 5, which were not seen here [13]. Therefore, it seems likely that BCL-2 expression in NCMT-1 cells is regulated by an alternative route, independent of LYN and MDS1/EVI1.

ABT-737 displayed a significant synergistic effect in killing NCMT-1 and K562 cells when combined with TKI. Although ABT-737 is not suitable for clinical practice due to poor physiochemical and pharmaceutical properties [38], the closely related Navitoclax (ABT-263), which is orally bioavailable, is in clinical development [37,39]. ABT-263 is already demonstrating promising results in lymphoid and other malignancies, providing optimism that these reagents will rapidly become clinically available for combination studies [40,41]. In NCMT-1 cells, the potent effects of the TKI + ABT-737 combination might be due to its relatively high expression of BCL-2. However,

it should be noted that ABT-737 alone had very limited effects, indicating that overcoming high levels of BCL-2 alone is insufficient to cause efficient cell death. The fact that this potent synergy was also observed in K562 cells, which are sensitive to TKI, and that BCL-2 and BCL-xL (which are the main targets of ABT-737 and ABT-263), are frequently overexpressed in advanced stage of CML [1,17], indicates that this combination would be beneficial in various stages of CML progression to improve clinical outcome. Furthermore, the fact that the synergistic effect was observed with low concentrations of both drugs might also indicate an advantage in terms of reducing drug usage to improve safety and efficacy, although clearly further investigation is warranted.

The molecular consequence of the TEL/MDS1/EVI1 fusion has not been fully resolved to date, probably due to its relative rarity [22]. As observed in the NCMT-1 cells, break points of the fusion are located on Exon 2 of *TEL*, *MDS1* and Exon 2 of *EVI1*, thus the ETS domain and DNA binding site of the TEL gene are absent in the fusion gene [42]. In contrast, the fusion gene does contain the two zinc finger motifs of the *EVI1* gene, and so the function of the *TEL/MDS1/EVI1* fusion likely reflects that of *EVI1* [43]. The siEVI1s suppressed the MDS1/EVI1 fusion to a greater extent than the EVI1 protein. Our data indicate that the overexpression of MDS1/EVI1 is able to regulate the phosphorylation status, and thereby likely the activity of AKT, which is coincident with a recent report that indicates EVI1 represses PTEN and activates the phosphoinositide 3-kinase/AKT pathway [36]. Interestingly, although the MDS1/EVI1 fusion was expressed at a far higher level than the EVI1 protein, and we observed a greater effect of the siRNA on reducing its expression a recent report indicated that EVI1 expression was more relevant to clinical outcome compared to MDS1/EVI1 expression [18]. Therefore, it remains possible that the effects we observed were related to reduction in EVI1 expression. Unfortunately, we are currently unable to modulate the expression of these two proteins differentially. Irrespective, the hypothesis that follows is that targeting AKT could be a rational treatment strategy for EVI1-positive tumors. Several AKT inhibitors are in development and/or currently undergoing clinical investigation [44], making this a realistic ambition. Furthermore, considering the increased frequency of this aberration following TKI treatment [45], additional investigation of this transcription factor and its related fusion proteins is warranted, particularly in terms of their regulation of apoptosis and the potential sensitization with ABT-737 or AKTi.

Our findings, although derived from a single cell line, have clear relevance in terms of the molecular basis of disease progression and BCR/ABL-independent TKI resistance in CML and the function of dysregulated EVI1 in tumor cells. In particular, the association of the overexpression of MDS1/EVI1 with the regulation of apoptosis has not been previously appreciated, and our findings that these proteins suppress the function of BAD via the AKT pathway and targeting phosphorylated AKT mimics the inhibition of EVI1 are novel. Furthermore, advanced-stage CML is currently largely intractable, and our findings that BH3-mimetics synergize with TKI, even in TKI-insensitive cells, warrant further evaluation, including clinically, in the near future.

Funding disclosure

The authors gratefully acknowledge the Daiichi-Sankyo Foundation for Life Sciences for a grant to K.S., Grant-Aid for Scientific Research (B) 22390192 and a Health Labour Sciences Research Grant H22YE010-01 for T.N., and the Association for International Cancer Research (AICR) for a grant to M.S.C. and C.K.H.

Acknowledgments

We would like to thank Dr. Ryohei Tanizaki for assistance with cell-line establishment, Kunihiko Takeyama, M.D., Ph.D. (Dana-Faber Cancer Institute, Boston, MA, USA) for providing the SU-DHL4 cell line, Kiyosumi Shibata, M.D., Ph.D. for providing the SK-OV3 cell line, Yoshitsugu Koyama, M.D. and Hiroshi Kosugi, M.D., Ph.D. (Ogaki Municipal Hospital, Ogaki, Japan) and Akio Kohno M.D., Ph.D. (JA Aichi Konan Kosei Hospital, Konan, Japan) for providing samples and information relating to this patient and Dr. A Hayden for assistance with synergy calculations.

Author contributions: K.S., A.T., Y.M., M.S.C., and T.N. designed research and analyzed results. K.S. and C.K.H. performed experiments. A.A. established the cell line. K.S. and M.S.C. wrote the manuscript. A.T., Y.M., and T.N. edited the manuscript. H.K., M.S.C., and T.N. supervised research. All the authors approved the final version of manuscript.

Conflict of interest disclosure

No financial interest/relationships with financial interest relating to the topic of this article have been declared.

References

1. Melo JV, Barnes DJ. Chronic myeloid leukaemia as a model of disease evolution in human cancer. Nat Rev Cancer. 2007;7:441–453.
2. Sawyers CL, McLaughlin J, Witte ON. Genetic requirement for Ras in the transformation of fibroblasts and hematopoietic cells by the Bcr-Abl oncogene. J Exp Med. 1995;181:307–313.
3. Skorski T, Kanakaraj P, Nieborowska-Skorska M, et al. Phosphatidylinositol-3 kinase activity is regulated by BCR/ABL and is required for the growth of Philadelphia chromosome-positive cells. Blood. 1995;86:726–736.
4. Druker BJ, Sawyers CL, Kantarjian H, et al. Activity of a specific inhibitor of the BCR-ABL tyrosine kinase in the blast crisis of chronic myeloid leukemia and acute lymphoblastic leukemia with the Philadelphia chromosome. N Engl J Med. 2001;344:1038–1042.
5. Kantarjian H, Giles F, Wunderle L, et al. Nilotinib in imatinib-resistant CML and Philadelphia chromosome-positive ALL. N Engl J Med. 2006;354:2542–2551.
6. Talpaz M, Shah NP, Kantarjian H, et al. Dasatinib in imatinib-resistant Philadelphia chromosome-positive leukemias. N Engl J Med. 2006; 354:2531–2541.

7. O'Brien SG, Guilhot F, Larson RA, et al. Imatinib compared with interferon and low-dose cytarabine for newly diagnosed chronic-phase chronic myeloid leukemia. N Engl J Med. 2003;348:994–1004.
8. Horowitz MM, Rowlings PA, Passweg JR. Allogeneic bone marrow transplantation for CML: a report from the International Bone Marrow Transplant Registry. Bone Marrow Transplant. 1996;17(suppl 3):S5–S6.
9. Diamond JM, Melo JV. Mechanisms of resistance to BCR-ABL kinase inhibitors. Leuk Lymphoma. 2011;52(suppl 1):12–22.
10. Apperley JF. Part I: mechanisms of resistance to imatinib in chronic myeloid leukaemia. Lancet Oncol. 2007;8:1018–1029.
11. Widmer N, Colombo S, Buclin T, Decosterd LA. Functional consequence of MDR1 expression on imatinib intracellular concentrations. Blood. 2003;102:1142.
12. Mahon FX, Belloc F, Lagarde V, et al. MDR1 gene overexpression confers resistance to imatinib mesylate in leukemia cell line models. Blood. 2003;101:2368–2373.
13. Dai Y, Rahmani M, Corey SJ, Dent P, Grant S. A Bcr/Abl-independent, Lyn-dependent form of imatinib mesylate (STI-571) resistance is associated with altered expression of Bcl-2. J Biol Chem. 2004;279:34227–34239.
14. Donato NJ, Wu JY, Stapley J, et al. BCR-ABL independence and LYN kinase overexpression in chronic myelogenous leukemia cells selected for resistance to STI571. Blood. 2003;101:690–698.
15. Holyoake T, Jiang X, Eaves C, Eaves A. Isolation of a highly quiescent subpopulation of primitive leukemic cells in chronic myeloid leukemia. Blood. 1999;94:2056–2064.
16. Holyoake TL, Jiang X, Jorgensen HG, et al. Primitive quiescent leukemic cells from patients with chronic myeloid leukemia spontaneously initiate factor-independent growth in vitro in association with up-regulation of expression of interleukin-3. Blood. 2001;97:720–728.
17. Radich JP. The biology of CML blast crisis. Hematology Am Soc Hematol Educ Program. 2007;384–391.
18. Barjesteh van Waalwijk van Doorn-Khosrovani S, Erpelinck C, van Putten WL, et al. High EVI1 expression predicts poor survival in acute myeloid leukemia: a study of 319 de novo AML patients. Blood. 2003; 101:837–845.
19. Mitani K, Ogawa S, Tanaka T, et al. Generation of the AML1-EVI-1 fusion gene in the t(3;21)(q26;q22) causes blastic crisis in chronic myelocytic leukemia. EMBO J. 1994;13:504–510.
20. Ogawa S, Kurokawa M, Mitani K, Yazaki Y, Hirai H. Overexpression of Evi-1 and dysmegakaryopoiesis in human leukemias: reply to Carapeti, Goldman and Cross, Leukemia 1996;10:1561. Leukemia. 1996;10:1849.
21. Suzukawa K, Parganas E, Gajjar A, et al. Identification of a breakpoint cluster region 3' of the ribophorin I gene at 3q21 associated with the transcriptional activation of the EVI1 gene in acute myelogenous leukemias with inv(3)(q21q26). Blood. 1994;84:2681–2688.
22. Nakamura Y, Nakazato H, Sato Y, Furusawa S, Mitani K. Expression of the TEL/EVI1 fusion transcript in a patient with chronic myelogenous leukemia with t(3;12)(q26;p13). Am J Hematol. 2002;69:80–82.
23. Goyama S, Yamamoto G, Shimabe M, et al. Evi-1 is a critical regulator for hematopoietic stem cells and transformed leukemic cells. Cell Stem Cell. 2008;3:207–220.
24. Kurokawa M, Mitani K, Irie K, et al. The oncoprotein Evi-1 represses TGF-beta signalling by inhibiting Smad3. Nature. 1998;394:92–96.
25. Kurokawa M, Mitani K, Yamagata T, et al. The evi-1 oncoprotein inhibits c-Jun N-terminal kinase and prevents stress-induced cell death. EMBO J. 2000;19:2958–2968.
26. Tanaka T, Nishida J, Mitani K, Ogawa S, Yazaki Y, Hirai H. Evi-1 raises AP-1 activity and stimulates c-fos promoter transactivation with dependence on the second zinc finger domain. J Biol Chem. 1994; 269:24020–24026.
27. Baccarani M, Cortes J, Pane F, et al. Chronic myeloid leukemia: an update of concepts and management recommendations of European LeukemiaNet. J Clin Oncol. 2009;27:6041–6051.
28. Atsumi A, Tomita A, Kiyoi H, Naoe T. Histone deacetylase 3 (HDAC3) is recruited to target promoters by PML-RARalpha as a component of the N-CoR co-repressor complex to repress transcription in vivo. Biochem Biophys Res Commun. 2006;345:1471–1480.
29. Chan HT, Hughes D, French RR, et al. CD20-induced lymphoma cell death is independent of both caspases and its redistribution into triton X-100 insoluble membrane rafts. Cancer Res. 2003;63:5480–5489.
30. Minami Y, Kiyoi H, Yamamoto Y, et al. Selective apoptosis of tandemly duplicated FLT3-transformed leukemia cells by Hsp90 inhibitors. Leukemia. 2002;16:1535–1540.
31. Cragg MS, Howatt WJ, Bloodworth L, Anderson VA, Morgan BP, Glennie MJ. Complement mediated cell death is associated with DNA fragmentation. Cell Death Differ. 2000;7:48–58.
32. Hiraga J, Tomita A, Sugimoto T, et al. Down-regulation of CD20 expression in B-cell lymphoma cells after treatment with rituximab-containing combination chemotherapies: its prevalence and clinical significance. Blood. 2009;113:4885–4893.
33. Peeters P, Wlodarska I, Baens M, et al. Fusion of ETV6 to MDS1/EVI1 as a result of t(3;12)(q26;p13) in myeloproliferative disorders. Cancer Res. 1997;57:564–569.
34. Kuroda J, Puthalakath H, Cragg MS, et al. Bim and Bad mediate imatinib-induced killing of Bcr/Abl+ leukemic cells, and resistance due to their loss is overcome by a BH3 mimetic. Proc Natl Acad Sci U S A. 2006;103:14907–14912.
35. Oltersdorf T, Elmore SW, Shoemaker AR, et al. An inhibitor of Bcl-2 family proteins induces regression of solid tumours. Nature. 2005;435: 677–681.
36. Yoshimi A, Goyama S, Watanabe-Okochi N, et al. Evi1 represses PTEN expression and activates PI3K/AKT/mTOR via interactions with polycomb proteins. Blood. 2011;117:3617–3628.
37. Cragg MS, Harris C, Strasser A, Scott CL. Unleashing the power of inhibitors of oncogenic kinases through BH3 mimetics. Nat Rev Cancer. 2009;9:321–326.
38. Vogler M, Dinsdale D, Dyer MJ, Cohen GM. Bcl-2 inhibitors: small molecules with a big impact on cancer therapy. Cell Death Differ. 2009;16:360–367.
39. Tse C, Shoemaker AR, Adickes J, et al. ABT-263: a potent and orally bioavailable Bcl-2 family inhibitor. Cancer Res. 2008;68:3421–3428.
40. Wilson WH, O'Connor OA, Czuczman MS, et al. Navitoclax, a targeted high-affinity inhibitor of BCL-2, in lymphoid malignancies: a phase 1 dose-escalation study of safety, pharmacokinetics, pharmacodynamics, and antitumour activity. Lancet Oncol. 2010;11:1149–1159.
41. Gandhi L, Camidge DR, Ribeiro de Oliveira M, et al. Phase I study of Navitoclax (ABT-263), a novel Bcl-2 family inhibitor, in patients with small-cell lung cancer and other solid tumors. J Clin Oncol. 2011;29: 909–916.
42. Bohlander SK. ETV6: a versatile player in leukemogenesis. Semin Cancer Biol. 2005;15:162–174.
43. Goyama S, Kurokawa M. Pathogenetic significance of ecotropic viral integration site-1 in hematological malignancies. Cancer Sci. 2009; 100:990–995.
44. Hirai H, Sootome H, Nakatsuru Y, et al. MK-2206, an allosteric Akt inhibitor, enhances antitumor efficacy by standard chemotherapeutic agents or molecular targeted drugs in vitro and in vivo. Mol Cancer Ther. 2010;9:1956–1967.
45. Paquette RL, Nicoll J, Chalukya M, et al. Frequent EVI1 translocations in myeloid blast crisis CML that evolves through tyrosine kinase inhibitors. Cancer Genet. 2011;204:392–397.

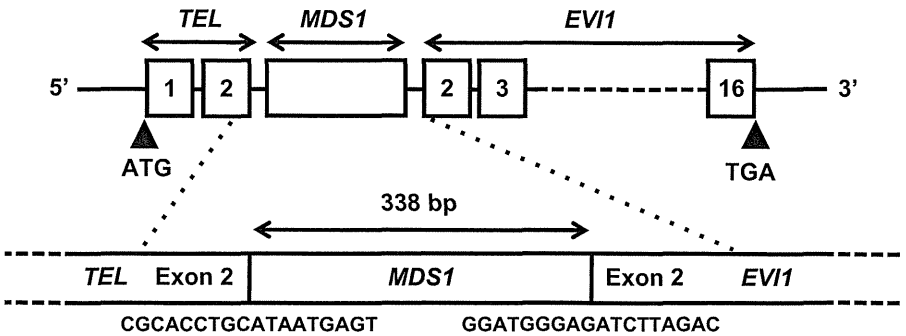

Supplementary Figure E1. Structure of the *TEL/MDS1/EVI1* fusion. A schematic representation of the *TEL/MDS1/EVI1* fusion present in the NCMT-1 cells is shown. Sequencing analysis revealed the break points of the fusion to be between Exon2 of *TEL*, *MDS1* and Exon2 of *EVI1*. This structure of the fusion gene corresponds to that reported previously [33].

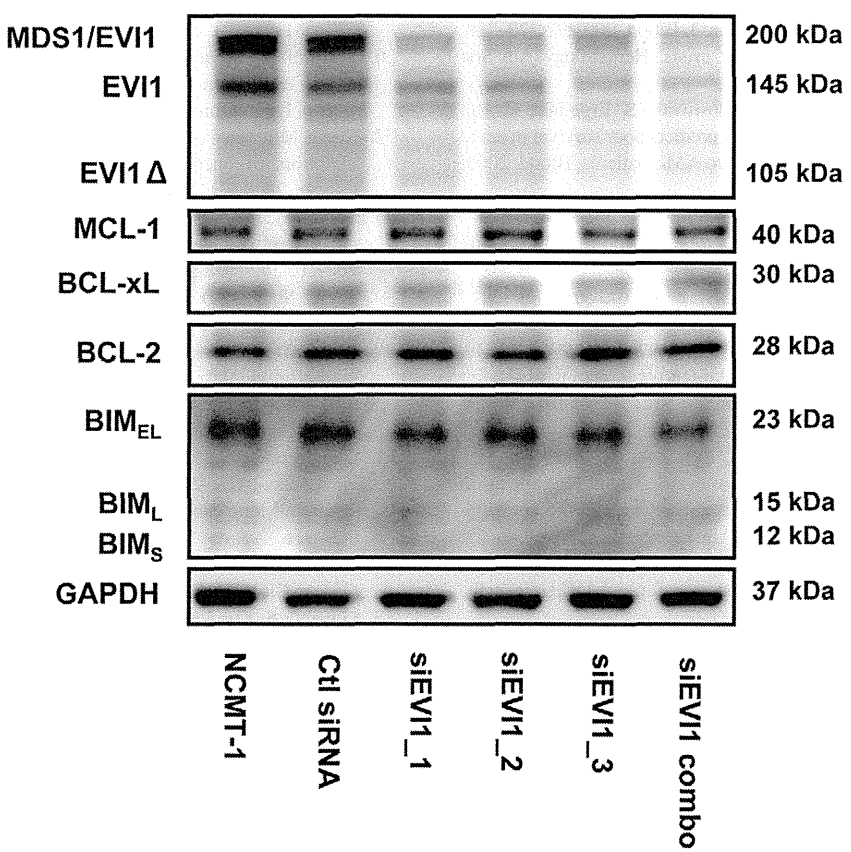

Supplementary Figure E2. MDS1/EVI1 knockdown does not affect the expression of BCL-2, BCL-xL, MCL-1, or BIM in NCMT-1 cells. Whole cell lysates were obtained 48 h after nucleofection of NCMT-1 cells with the siRNA indicated. Immunoblotting for MDS1/EVI1, BIM, BCL-2, BCL-xL, MCL-1, and glyceraldehyde phosphate dehydrogenase (GAPDH) as a loading control was then performed. BCL-2 and BIM expression were not changed by the suppression of MDS1/EVI1, indicating it does not regulate these apoptotic-related proteins. All of the images except for BCL-xL and MCL-1 were obtained from the same membrane. The BCL-xL and MCL-1 blot were taken from the same membrane.

Supplementary Table E1. Primer list

Name	Sequence	Annealing temperature (°C)	Cycles
TEL-U	5′-ATG TCT GAG ACT CCT GCT CA-3′	58	35
EVI1-U	5′-TGG AGA GCA GAT CCT AGA GA-3′	58	35
EVI1-L	5′-CAC AGT CTT CGC AGC GAT AT-3′	58	35
β-actin U	5′-TCA CTC ATG AAG ATC CTC A-3′	58	35
β-actin L	5′-TTC GTG GAT GCC ACA GGA C-3′	58	35

Supplementary Table E2. Source of primary antibodies for immunoblotting

Antibody	Source	Location
BCR-ABL (8E9)	BD Biosciences Pharmingen	San Diego, CA, USA
EVI1 (#2593)	Cell Signaling Technology (CST)	Danvers, MA, USA
pBCR-ABL (Tyr245) (#2861)	CST	Danvers, MA, USA
pCrkL (Tyr207) (#3181)	CST	Danvers, MA, USA
pSTAT5 (#9359)	CST	Danvers, MA, USA
STAT5 (#9358)	CST	Danvers, MA, USA
pERK1/2	CST	Danvers, MA, USA
ERK1/2	CST	Danvers, MA, USA
pAKT (Ser473) (#4060)	CST	Danvers, MA, USA
AKT (#9272)	CST	Danvers, MA, USA
pBAD (Ser136) (#4366)	CST	Danvers, MA, USA
BIM (#2819)	CST	Danvers, MA, USA
BIM	Enzo Life Sciences	Exeter, UK
BAD	Enzo Life Sciences	Exeter, UK
BCL-2	BD Biosciences Pharmingen	San Diego, CA, USA
BCL-2	CST	Danvers, MA, USA
BCL-xL	CST	Danvers, MA, USA
BCL-xL	BD Biosciences Pharmingen	San Diego, CA, USA
MCL-1	Abcam	Cambridge, UK
MCL-1 (#4572)	CST	Danvers, MA, USA
PTEN	Millipore	Billerica, MA, USA
GAPDH (6C5)	Abcam	Cambridge, UK